

MODIFICATION OF PHENYTOIN CRYSTALS: INFLUENCE OF  
3-PROPANOYLOXYMETHYL-5,5-DIPHENYLHYDANTOIN ON SOLUTION-  
PHASE CRYSTALLIZATION AND RELATED CRYSTAL PROPERTIES

by

JOHN DAVID GORDON

B. Sc. (Hons.), Dalhousie University, 1988

A THESIS SUBMITTED IN PARTIAL FULFILMENT OF  
THE REQUIREMENTS FOR THE DEGREE OF  
MASTER OF SCIENCE

in

THE FACULTY OF GRADUATE STUDIES

Faculty of Pharmaceutical Sciences

(Division of Pharmaceutics and Biopharmaceutics)

We accept this thesis as conforming  
to the required standard

THE UNIVERSITY OF BRITISH COLUMBIA

September 1991

© John David Gordon, 1991

721

In presenting this thesis in partial fulfilment of the requirements for an advanced degree at the University of British Columbia, I agree that the Library shall make it freely available for reference and study. I further agree that permission for extensive copying of this thesis for scholarly purposes may be granted by the head of my department or by his or her representatives. It is understood that copying or publication of this thesis for financial gain shall not be allowed without my written permission.

Department of PHARMACEUTICAL SCIENCES

The University of British Columbia  
Vancouver, Canada

Date OCTOBER 8, 1991

## ABSTRACT

Recent studies in our laboratory have demonstrated that doping of phenytoin (5,5-diphenylhydantoin; DPH) crystals with traces of 3-acetoxymethyl-5,5-diphenylhydantoin, AMDPH, during growth from methanol consistently modifies their physical properties e.g., habit, energy, surface area, dissolution rate (Chow and Hsia, 1991). AMDPH is a suggested ester prodrug of DPH (Varia et al., 1984). In addition to being structurally akin to DPH, AMDPH is not appreciably greater in molecular size than DPH, which makes possible, from the thermodynamic standpoint, the incorporation of AMDPH into the crystal lattice of DPH. To investigate how the molecular sizes of the ester homologues of DPH influence their incorporation into DPH crystals and the resulting crystal properties, studies similar to those described above have been applied to another additive higher in the ester homologous series, viz. 3-propanoyloxymethyl-5,5-diphenylhydantoin (PMDPH) (Gordon and Chow, 1991). PMDPH, also cited as a prodrug candidate of DPH, differs from AMDPH in possessing an additional methylene group in its ester side chain (Varia et al., 1984).

The effects of recrystallizing DPH from methanol under defined conditions in the presence of various concentrations of PMDPH were investigated. An increase in the concentrations of PMDPH (from 0.5 to 11 gL<sup>-1</sup>) in the crystallization solutions at 30 °C brought about a linear increase in PMDPH sorption (0.03-0.57 mole %) by the DPH crystals, a morphological change of the crystal from needles to elongated plates, a drop in crystallization yield, a decrease in particle size and an increase in specific surface area of the crystals. Vigorous multiple washing of the doped crystals with methanol/water (5:95) detached ~ 70 ± 2 %w/w of PMDPH and a negligible amount of DPH (1.0 ± 0.1

%w/w), indicating that the additive was predominantly adsorbed on the crystal surface. While powder X-ray diffraction studies on the doped and pure crystals presented no significant differences in both their diffraction patterns and lattice spacings, the enthalpy of fusion,  $\Delta H^f$ , and entropy of fusion,  $\Delta S^f$ , of the crystals, as determined by differential scanning calorimetry, were lowered with increasing sorption of PMDPH (by as much as 8 % at 0.57 mole % of PMDPH), indicating that the sorption of PMDPH raised both the enthalpy and entropy of the crystals. The disruption index of PMDPH, as estimated from the negative slope of the linear regression of  $\Delta S^f$  on the ideal entropy of mixing,  $\Delta S_{ideal}$ , was  $19 \pm 2$ , implying an introduction of considerable disorder and disruption (about 19 times that expected from pure random mixing alone) in the crystal lattice of DPH by the presence of PMDPH. Determination of the dissolution rate of the various samples at 25 ° and 37 °C afforded an upward trend in initial dissolution rate (IR) as a function of the PMDPH sorption, with the largest increase at 0.36 mole % of PMDPH (~3.3 times those of the pure, undoped crystals). The intrinsic dissolution rate, IDR (i.e., IR divided by initial surface area), of the crystals at both temperatures also displayed a rise, but peaked at 0.16 mole % of sorbed PMDPH (corresponding to ~1.7 fold increase). The observed increases in IDR are probably mediated through increases in the concentration of crystal defects arising from the sorption of PMDPH, and to a much lesser extent, through changes in crystal habit.

## TABLE OF CONTENTS

	Page
Abstract	ii
Table of contents	iv
List of Tables	viii
List of Figures	ix
List of Abbreviations	xii
Acknowledgements	xvi
 1 INTRODUCTION	
1.1 Rationale for the study	1
1.2 Crystal habit	2
1.2.1 Mechanisms of growth	3
1.2.1.1 Surface energy theories	3
1.2.1.2 Diffusion theories	3
1.2.1.3 Adsorption layer theories	6
1.2.2 Effect of impurities / additives on crystal growth	8
1.2.3 Pharmaceutical significance of crystal habit	11
1.2.3.1 Effect on mechanical properties	11
1.2.3.2 Effect on dissolution rate	12
1.3 Crystal defects	14
1.3.1 Classification of crystal defects	14
1.3.1.1 Point defects	14
1.3.1.2 Line defects	16
1.3.1.3 Plane defects	16
1.3.2 Formation of crystal defects	18

1.3.3	Formation of impurity defects and solid solutions	21
1.3.3.1	Substitutional solid solutions	21
1.3.3.2	Energetics of solid solutions	23
1.3.4	Pharmaceutical significance of crystal defects	24
1.3.4.1	Effect on processing characteristics	24
1.3.4.2	Effect on stability	26
1.3.4.3	Effect on dissolution rate	26
1.4	Dissolution of solids	27
1.4.1	Kinetics of dissolution	28
1.4.1.1	Transport-controlled dissolution	28
1.4.1.2	Surface-reaction controlled dissolution	29
1.4.1.3	Mixed surface-reaction and transport-controlled dissolution	30
1.4.2	Factors affecting dissolution	30
1.5	Phenytoin as a model	31
1.6	Crystal modification of phenytoin	34
1.6.1	Methyl ester prodrugs of DPH	35
1.7	Scope of study	36
2	Experimental	38
2.1	Materials	38
2.2	Equipment	40
2.3	Preparation and characterization of 3-propanoyloxymethyl-5,5-diphenylhydantoin (PMDPH)	42
2.3.1	Synthesis of PMDPH	42
2.3.2	Characterization of PMDPH	42
2.3.2.1	Differential scanning calorimetry	42
2.3.2.2	Solution $^1\text{H}$ -nmr spectroscopy	43

2.4	Batch crystallization of DPH from methanol	43
2.5	Determination of sorption of PMDPH by DPH crystals	44
2.6	Surface-absorbed additive determination	44
2.7	Determination of residual methanol content in DPH crystals	44
	2.7.1 Assay procedure	44
	2.7.2 Gas chromatographic conditions	45
2.8	Powder X-ray diffraction	45
2.9	Scanning electron microscopy	46
2.10	Particle size distribution	46
2.11	Specific surface area measurements	46
2.12	Differential scanning calorimetry	48
2.13	Solubility of PMDPH-doped DPH crystals in water	48
2.14	Dissolution studies	49
3	Results and discussion	50
3.1	Preparation of PMDPH	50
	3.1.1 Synthesis	50
	3.1.2 Characterization	51
3.2	Characterization of DPH crystals grown from methanol	51
	3.2.1 Crystal morphology, particle size and crystallization yield	51
	3.2.2 Retention of methanol by DPH crystals	61
	3.2.3 Sorption of PMDPH by DPH crystal	63
	3.2.4 Powder X-ray diffraction analysis	65
	3.2.5 Thermal analysis	69
	3.2.5.1 Thermodynamic interpretation	69
	3.2.6 Dissolution studies	76
	3.2.6.1 Dissolution behavior of PMDPH-doped DPH	

	samples	76
	3.2.6.2 Effect of stirring speed on dissolution rate	82
	3.2.6.3 Comparison with AMDPH-doped DPH	
	samples	84
4	Conclusions	85
5	Suggestions for future studies	87
6	References	89



## LIST OF TABLES

	Page
1. Equilibrium solubility of DPH crystals grown from methanol containing various concentrations of PMDPH in water at 30 °C.	68
2. Thermal analysis data of DPH crystallized from methanol containing various concentrations of PMDPH.	72

## LIST OF FIGURES

	Page
1. Three possible adsorption sites on a growing crystal face for additives/impurities (from Davies, 1976).	10
2. Three types of point defects (from Mullin, 1972).	15
3. An edge dislocation (from Moore, 1972).	17
4. A screw dissolution (from Mullin, 1972).	17
5. A stacking fault (from Hull and Bacon, 1984).	19
6. A twinned structure where x-y is the trace of the twin composite plane (from Hull and Bacon, 1984).	19
7. A grain boundary (from Mullin, 1972).	20
8. Free energy of a crystal, $G_{\text{cry}}$ , as a function of the number of impurity defects, the contribution of the change in enthalpy and entropy resulting from lattice defects, and the contribution of the ideal entropy of mixing (modified from Swalin, 1962).	25
9. Chemical structure of phenytoin (5,5-diphenylhydantoin; DPH).	33
10. Chemical structures of 3-hydroxymethyl-5,5-diphenylhydantoin and various methyl ester derivatives.	33
11. 400 MHz $^1\text{H}$ -NMR spectrum of PMDPH.	52
12. Scanning electron photomicrograph of DPH crystallized from methanol in the absence of PMDPH.	53
13. Scanning electron photomicrograph of DPH crystallized from methanol in the presence of $1 \text{ g L}^{-1}$ PMDPH.	54
14. Scanning electron photomicrograph of DPH crystallized from methanol in the presence of $3 \text{ g L}^{-1}$ PMDPH.	55

15. Scanning electron photomicrograph of DPH crystallized from methanol in the presence of  $5 \text{ g L}^{-1}$  PMDPH. 56
16. Scanning electron photomicrograph of DPH crystallized from methanol in the presence of  $7 \text{ g L}^{-1}$  PMDPH. 57
17. Specific surface areas of DPH crystallized from methanol containing various concentrations of PMDPH. Each data point is the mean value of 2 separate batches. 59
18. Yields of DPH crystallized from methanol containing various concentrations of PMDPH. 60
19. Linear regression plot of the solubility of three methyl esters of DPH in methanol at  $30^\circ\text{C}$  against their respective melting points. 62
20. Sorption of PMDPH by DPH crystals grown from methanol containing various concentrations of PMDPH. 64
21. Powder X-ray diffraction pattern of DPH crystals grown from methanol containing (A)  $0 \text{ g L}^{-1}$  PMDPH; and (B)  $11 \text{ g L}^{-1}$  PMDPH. 67
22. Differential scanning calorimetric thermograms of DPH crystals grown from methanol containing (A)  $0 \text{ g L}^{-1}$  PMDPH; and (B)  $7 \text{ g L}^{-1}$  PMDPH. 70
23. Enthalpies of fusion of DPH crystals grown from methanol in the presence of various concentrations of PMDPH. 71
24. Linear regression plot of the entropy of fusion against the ideal molar entropy of mixing for DPH crystals grown from methanol in the presence of various concentrations of PMDPH. 75
25. Dissolution-time profiles at  $25^\circ\text{C}$  of DPH crystals grown from methanol in the presence of various concentrations of PMDPH. 77
26. Dissolution-time profiles at  $37^\circ\text{C}$  of DPH crystals grown from

	methanol in the presence of various concentrations of PMDPH.	78
27.	Initial dissolution rates at 25 °C and 37 °C and at 100 and 200 rpm of DPH crystals grown from methanol in the presence of various concentrations of PMDPH.	79
28.	Intrinsic dissolution rates at both 25 °C and 37 °C and at 100 rpm of DPH crystals grown from methanol containing various concentrations of PMDPH.	81
29.	Effect of stirring speed on the intrinsic dissolution rate of DPH crystals grown from methanol containing 0,1 and 5 g L <sup>-1</sup> of PMDPH.	83

## LIST OF ABBREVIATIONS AND SYMBOLS

Å	angstrom
a	dimension of crystallographic unit cell along x-axis
A	surface area
AMDPH	3-acetoxymethyl-5,5-diphenylhydantoin
b	dimension of crystallographic unit cell along y-axis
BMDPH	3-butanoyloxymethyl-5,5-diphenylhydantoin
c	dimension of crystallographic unit cell along z-axis
C	constant related to the enthalpy of adsorption
C*	concentration of solute in the bulk of a supersaturated solution
°C	degrees celsius
C <sub>i</sub>	concentration of solute at surface of the solid
C <sub>s</sub>	concentration of solute in a saturated solution
D	diffusion coefficient of a solute
DPH	phenytoin
g	gram
µg	microgram
ΔG	Gibbs free energy
GC	gas chromatography
G <sub>cry</sub>	Gibbs free energy of crystal
G <sub>perf</sub>	Gibbs free energy of the hypothetical perfect crystal
h	thickness of film layer
ΔH <sup>f</sup>	change in enthalpy upon fusion
H <sub>liquid</sub>	enthalpy of the liquid phase
HMDPH	3-hydroxymethyl-5,5-diphenylhydantoin

HPLC	high performance liquid chromatography
$H_{\text{solid}}$	enthalpy of the solid phase
IDR	intrinsic dissolution rate
$k$	Boltzmann constant
$k_d$	coefficient of mass transfer by diffusion
kg	kilogram
$k_o$	over-all rate constant
$k_{\text{obs}}$	observed rate constant
$k_r$	rate constant for solute incorporation
$k_t$	coefficient of mass transfer
L	litre
$\mu\text{L}$	microlitre
m	metre
$\text{m}^2$	square metre
$\mu\text{m}$	micrometre
mg	milligram
MHz	megahertz
min	minute
mL	millilitre
mol	mole
N	number of host molecules in a crystal
n	number of impurity molecules in a crystal
P	partial pressure of the adsorbate
$P_o$	saturated vapor pressure of the adsorbate
PEG	polyethylene glycol
PMDPH	3-propanoyloxymethyl-5,5-diphenylhydantoin
ppm	parts per million

PVP	polyvinylpyrrolidone
q	quartet
r	volume of overlapping parts of two superimposed molecules
R	growth rate
rpm	revolutions per minute
$\sigma$	relative supersaturation
$\Sigma$	coefficient of geometrical similarity
$s'$	$C^* / C_s$
s	singlet
S	specific surface area
SEM	scanning electron microscopy
$\Delta S^f$	change in entropy upon fusion
$\Delta S^f_o$	hypothetical entropy of fusion of perfect crystal
$\Delta S_{ideal}$	ideal molar entropy of mixing
$S_j$	partial molar entropy of component j
$S_{liquid}$	entropy of the liquid phase
$S_{solid}$	entropy of the solid phase
T	volume of non-overlapping parts of two superimposed molecules
t	triplet or time
T	absolute temperature
$\Delta U^f$	change in internal energy upon fusion
UHP	ultra high purity
$U_{liquid}$	internal energy of the liquid phase
$U_{solid}$	internal energy of the solid phase
UV	ultraviolet

$\Delta V^f$	change in molar volume upon fusion
$V_{\text{liquid}}$	molar volume of the liquid phase
$V_{\text{solid}}$	molar volume of the solid phase
$w$	weight of krypton adsorbed
$w_m$	weight of hypothetical adsorbed layer
$w/w$	weight / weight
$x$	mole fraction
$Z$	number of molecules in a crystallographic unit cell



## ACKNOWLEDGEMENTS

I would like to thank my supervisor, Dr. Albert Chow, for his guidance and encouragement throughout the course of this study. I am also grateful to the members of my research committee, Dr. F. Abbott, Dr. H. Burt, Dr. J. Diamond and Dr. A. Mitchell for their time and guidance. I would like to thank Dr. W. Riggs and A. Szeitz for their work on the gas chromatographic analysis of methanol. I am also grateful to my basement co-workers, Ron Aoyama, Seema Gadkari, Carlos Hsia and John Jackson for their never ending assistance and support. Financial support from the British Columbia Medical Services Foundation and Berlex Laboratories Inc. is gratefully acknowledged. Finally, I am very grateful to my wife, Darlene, and my son, Jacob, for their constant love and encouragement.

## 1. INTRODUCTION

### 1.1 Rationale for the study

Batch-to-batch variations in the physical properties of pharmaceutical solids can result in serious formulation problems such as bioinequivalence, suboptimal bioavailability, tableting failure as well as chemical and physical instability of the solid drugs in their final dosage forms (Haleblian and McCrone, 1969; Haleblian, 1975; York, 1983). Although it is commonly recognized that these variations are often a result of changes in crystal structure, crystal habit and / or in the degree of crystal imperfections, the mechanisms by which these properties exert their influences are not well understood. As a result, many interbatch problems are either neglected or solved empirically. This situation is unlikely to improve unless researchers can develop a better understanding of the causes and consequences of the variation of these properties.

Among these properties, crystal structure is probably the most widely studied and best understood in terms of its relationship to pharmaceutical properties. It has long been known that the crystal structure of a material plays an important role in determining its processability, stability, solubility, dissolution rate and bioavailability. As a result, the more energetic form of a material will have a higher activity and hence a greater solubility and dissolution rate (Higuchi et al., 1963). This fact may be exploited to overcome solubility or dissolution related problems of solid pharmaceuticals if a more energetic form (e.g., a metastable polymorph or solvate) of the material in question can be readily obtained. Failing this, other approaches such as solid dispersion in a water soluble carrier, grinding or melt quenching may be used to create a more energetic form of the substance.

While the production of these highly energetic forms may appear to provide a simple solution to solubility-related problems, there are caveats that must be kept in mind when dealing with unstable or metastable forms. As these forms are thermodynamically unstable, polymorphic transformation, phase separation and/or recrystallization can occur during processing or storage. This could result in changes in pharmaceutical properties such as dissolution rate and bioavailability.

The effects of crystal habit and crystal imperfections on pharmaceutical properties, although well documented, have not been completely elucidated. This is largely due to a lack of understanding of the mechanisms by which they exert their influences and partially to the availability of very few good or appropriate techniques for their study. Continued progress in the area of "crystal engineering" which deals with the prediction, control and exploitation of crystallization behavior of organic solids (Desiraju, 1987), however, is demonstrating its importance and utility. With this in mind, the goal of this study is to engineer drug crystals with optimal physical, biological and mechanical properties. This study attempts to achieve this goal through the use of synthetic additives related to the drug by structure to modify the crystal habit and / or crystal defects of drugs with a view to optimizing their physical characteristics (e.g., dissolution rate) in a predictable and reproducible fashion.

## 1.2 Crystal habit

The habit (i.e., morphology) of a crystal is determined primarily by the internal structure of the crystal. However, the environment of the growing crystal also plays a significant role in its development. In the case of crystal growth from solution, factors such as type of solvent, temperature, degree of supersaturation and the presence of impurities can all affect the growth and

consequently the habit of the product (Hartman, 1963; Mullin, 1972). In order to properly understand the development of the habit of a crystal, an examination of the mechanisms of crystal growth is essential.

#### 1.2.1 Mechanisms of crystal growth

Before the growth of a crystal from solution will begin, the system in question must first attain some degree of supersaturation which ultimately leads to nucleation and then to crystal growth. Mullin (1972) broadly classified the theories which address the mechanisms of crystal growth into the following three categories: (1) Surface energy theories; (2) Diffusion theories; and (3) Adsorption layer theories.

##### 1.2.1.1 Surface energy theories

Surface energy theories proceeded from the idea that the shape a growing crystal assumes is that which will have a minimum surface energy (Mullin, 1972). This notion was based on the knowledge that a fluid is most stable when it has a minimal surface area, and hence, a minimal surface free energy. However, the utility of these ideas has been questioned because of the basic differences in the internal arrangements between fluids and crystals. Furthermore, the surface energy approach cannot account for the effects of supersaturation or solution movement on crystal growth rate (Mullin, 1972) thus prompting the majority of workers in the area to lean toward alternative approaches to describe crystal growth behavior.

##### 1.2.1.2 Diffusion theories

The diffusion-based theories originated with the work of Noyes and Whitney (1897) who proposed that crystal growth may be considered to be the

reverse of dissolution and that both processes are diffusion-related.

Furthermore, the rates of both processes are related to the difference between the concentration of material at the solid surface and that in the bulk of the solution. The rate of growth may be defined as follows:

$$dm / dt = k_t A (C^* - C_s) \quad (1)$$

where  $dm / dt$  represents the amount of solid deposited per unit time,  $k_t$  is the coefficient of mass transfer,  $A$  is the surface area of the crystal,  $C^*$  is the concentration in the bulk of the supersaturated solution and  $C_s$  is the concentration of saturated solution.

Nernst (1904) modified equation (1) based on the assumption that there is a thin stagnant film of liquid adjacent to the crystal face through which the solute must diffuse in order to reach the growing face. This assumption allowed Nernst to express the coefficient of transfer ( $k_t$ ) as follows:

$$k_t = D / h \quad (2)$$

where  $D$  is the diffusion coefficient of the solute and  $h$  is the thickness of the film.

The inverse proportionality between the growth rate of the crystal and the thickness of the film suggests that the growth rate will increase upon decreasing film thickness. Therefore, one would expect a very large growth rate in a system with a high degree of agitation because the film thickness should decrease with increasing agitation. Since the growth rate of a crystal will not increase indefinitely with degree of agitation (Marc, 1908), the film diffusion approach is not a satisfactory description of the mechanism of crystal growth.

Berthoud (1912) and Valetton (1923, 1924) introduced significant changes to diffusion theory by suggesting that crystal growth proceeds via two steps, namely diffusion of the solute from the bulk of the solution to the solid surface and incorporation of the solute into the crystal lattice. These two steps are normally considered to be first order in nature and may be expressed as

$$(1) \quad dm / dt = k_d A (C^* - C_i) \quad (3)$$

and

$$(2) \quad dm / dt = k_r A (C_i - C_s) \quad (4)$$

where  $k_d$  represents a coefficient of mass transfer by diffusion,  $k_r$  is the rate constant for the solute incorporation and  $C_i$  is the concentration at the surface of the solid. If the system in which the crystal is growing remains unstirred, equation (3) could be used to describe the rate of growth. On the other hand, if there is a significant amount of agitation, the incorporation process (i.e., equation (4)) will control the growth rate.

The concentration of solute at the surface of the solid,  $C_i$ , is difficult to measure and, therefore, is often omitted from rate expressions. Instead, researchers consider an over-all driving force (i.e.,  $C^* - C_s$ ) and express the rate equation as

$$dm / dt = K_o A (C^* - C_s)^n \quad (5)$$

where  $n$  is the order of the over-all growth process and  $K_o$  is the over-all rate constant which accounts for both diffusion and solute incorporation, and may be expressed as

$$1 / K_o = 1 / k_d + 1 / k_r \quad (6)$$

if  $n = 1$  and the solute incorporation process is also first-order.

While diffusion theories have proven to be very useful for obtaining mathematical quantities which can be used to compare growth rates, they do have limitations, e.g., layer growth and defect-controlled growth cannot be properly explained by current diffusion theories. Some of these limitations may be more appropriately addressed by adsorption layer theories of crystal growth.

### 1.2.1.3 Adsorption layer theories

Volmer (1939) first suggested that crystal growth may proceed in a layer-by-layer fashion. Volmer's theory (or the Gibbs-Volmer theory) proposed that upon arriving at the surface of the growing crystal, the solute (atoms, ions or molecules) migrates freely along the surface creating an adsorbed layer of solute at the surface-solution interface. The solute in this layer remains in equilibrium with the solute in the bulk of the solution. These solute molecules eventually attach to the crystal lattice at the most favorable sites (i.e., active centres) until ultimately, under ideal conditions, the whole face (or layer) is complete. In order for growth to continue with a new layer, a 'centre of crystallization' must be created. Volmer's theory suggests that the creation of a two-dimensional nucleus on the surface will allow growth to proceed. This type of nucleation process is similar to the three-dimensional nucleation that must occur before growth from solution begins.

Kossel's (1934) theory differs from Volmer's in that Kossel suggests that the flat growing surface is divided into two regions by a monomolecular step. The solute molecules migrating along the surface will then tend to become attached at kink sites within the step. The kink will move along the step until the face is complete at which point two-dimensional nucleation must occur in order for growth to continue.

Both of the above propositions require the occurrence of two-dimensional nucleation on a complete surface before growth can proceed. Because two-dimensional nucleation will only occur if there is a relatively high degree of supersaturation in the region (Mullin, 1972) and because experimental evidence has demonstrated that many crystal faces will still grow quite readily at relatively low supersaturations (e.g., see Volmer and Schultz,

1931), the proposed dependence of crystal growth on surface nucleation would seem invalid at low supersaturations.

An alternate approach was proposed by Frank (1949) who suggested that growth could continue at any degree of supersaturation if screw dislocations, which are thermodynamically unstable one dimensional defects (see section 1.3.1), are present on the crystal face. The presence of screw dislocations will allow crystal faces to continue to grow up a 'spiral ramp or staircase' as if the surface were covered with kink sites without the need for surface nucleation; thus, growth will continue uninterrupted at a rate which should be close to the maximum for a given supersaturation.

In an effort to accurately predict rates of crystal growth, Burton, Cabrera and Frank (1951) developed a kinetic theory of growth which was based on the level of supersaturation and the screw dislocation mechanism of growth. Their proposals allowed researchers to calculate reasonable growth rates (at any supersaturation) which were much closer to experimentally observed rates than those calculated previously. Burton, Cabrera and Frank developed the following (BCF) relationship:

$$R = A\sigma^2 \tanh (B / \sigma) \quad (7)$$

where  $\sigma$  is the relative supersaturation,  $S' - 1$  (where  $S' = C^* / C_S$ ) and A and B are complex, temperature dependent constants which incorporate parameters dependent on step spacings. At low supersaturations, equation (7) approximates to  $R \propto \sigma^2$  while at high supersaturations  $R \propto \sigma$ . Thus, as the degree of supersaturation increases, the growth rate becomes a linear function of supersaturation.



### 1.2.2 Effects of impurities / additives on crystal growth

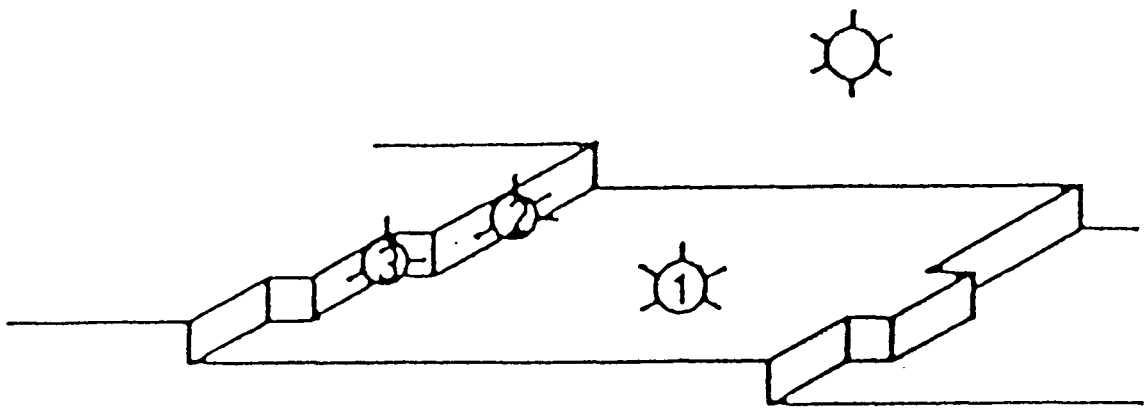
The habit of crystals grown from solution is dependent on a number of factors e.g., supersaturation, rate of cooling, degree of agitation, nature of the solvent and the presence of foreign substances (impurities or additives).

The presence of additives or impurities in the crystallization medium can substantially affect the growth kinetics of a material. If the additive affects some faces preferentially then a change in habit may result. The effects of additives can vary from total suppression to a significant enhancement of crystal growth, depending upon the type of interactions which occur between the crystallizing material, the additive and the solvent. Furthermore, the quantity of additive required to cause an effect varies from as little as  $10^{-9}$  mole fraction in some instances to relatively large concentrations in others (Berkovitch-Yellin, 1985). The effect of additives on crystal growth will depend on the quantity of additive present, the mechanism of the growth process (e.g., Volmer or Kossel's birth and spread process versus BCF process) and the degree of supersaturation of the solutions (Davey, 1979).

Additives may influence crystal growth from solutions in a variety of ways. For example, additives may alter the properties of the solution, change the physicochemical properties of the adsorption layer, or affect growth by adsorbing at sites on the growing faces (Davey, 1979). The first of these possibilities, alteration of the solution properties, could bring about a change in the equilibrium solubility of the crystallizing material, thereby altering the availability of growth sites. In the second instance, the additives may change the interfacial tension at the solid-solvent interface, thereby affecting the integration of growth units. For example, a decrease in the interfacial tension could: (1) increase the number of critical nuclei which can be formed per unit area and time which in turn will bring about an increase in growth rate if surface

nucleation is a requirement (e.g., for Volmer or Kossel's birth and spread approaches); or (2) decrease the step spacing of screw dislocations thus increasing growth rate (by Burton-Cabrera-Frank (BCF) approach). In the case of direct adsorption of the additive onto the growing face, the additive may adsorb at one of three possible sites (Fig. 1). The additive may adsorb at one of the energetically favoured kink sites which will increase the energy required to place a solute molecule in that site. Alternatively, the additive could occupy either a step site which would impede the rate and extent of advancement of the step or a ledge site which would result in a decrease in the diffusional flux toward the step.

There have been many reports demonstrating that the presence of impurities in the crystallization medium could significantly modify the habit of the recrystallizing material. For example, in the pharmaceutical literature, there have been several reports on the effect of additives on the crystal habit of adipic acid, a tablet lubricant (Michaels and Colville, 1960; Fairbrother and Grant, 1978, 1979; Chow et al., 1984). Michaels and Colville (1960) demonstrated that it was possible to reproducibly modify the habit of adipic acid crystals by recrystallization from water in the presence of ionic surfactants. Adipic acid crystallized from aqueous solution containing anionic surfactants developed in the form of long, thin needles while crystallization with cationic surfactants produced thin, flaky plates. Fairbrother and Grant (1978) further showed the feasibility of using trace amounts of additives to intentionally and reproducibly modify the crystal habit of adipic acid by recrystallizing the tablet lubricant from water containing small quantities of n-alkanoic acids or n-alkanols. The concentration of additive required to produce a significant effect ranged from only 2  $\mu\text{g}$  / mL for undecanoic acid to 2.5 mg / mL for hexanol. Fairbrother and



(1) Ledge site

(2) Step site

(3) Kink site

Fig. 1 Three possible adsorption sites on a growing crystal face for additives/impurities (from Davey, 1976).

Grant (1979) attributed the effect of the additive to selective adsorption of the additive onto specific faces of the growing crystals.

In a similar fashion, Chow et al. (1985) demonstrated that the principles established with adipic acid were also applicable to acetaminophen, a polyfunctional aromatic compound used in drug therapy as an analgesic and antipyretic. In their study, Chow et al. showed that the crystal habit and several other important physical properties of acetaminophen could be reproducibly altered by incorporating trace quantities of the additive, *p*-acetoxyacetanilide, into its crystal lattice during crystallization from aqueous solution. An increase in the concentrations of *p*-acetoxyacetanilide in the crystallization medium produced an approximately sigmoidal increase in the uptake of the additive into the growing crystals which in turn resulted in a progressive elongation of the crystal habit.

### 1.2.3 Pharmaceutical significance of crystal habit

#### 1.2.3.1 Effect on mechanical properties

Since the habit of crystals determines how they contact each other during processing, manufacturing properties ranging from a powder's flow characteristics to caking tendency (Mullin, 1972) are all affected by the habit of the crystals which constitute the powder. There have been numerous reports indicating that a change in the habit of a material can cause a change in the flow characteristics of the material (Higuchi and Simonelli, 1975; Jones, 1977; Lieberman and Latchman, 1980). For example, it has been noted that tolbutamide crystals in the shape of prisms exhibit better flow behavior than that of platy tolbutamide crystals, whose use leads to powder bridging in the hopper during tableting (Simmons et al.; 1972). Habit further affects the tableting of

materials by influencing properties such as particle slippage (York, 1978) and bonding (Alderborn and Nystrom, 1982) during compression. Furthermore, since habit also affects the packing density of pharmaceutical crystals (Ridgway and Rupp, 1969), it will also influence the uniformity of formulations including tablet weight (Ridgway and Shotton, 1970).

Problems associated with undesirable crystal habits are normally circumvented through additional processing such as milling or grinding; however, such processes are not only costly and time-consuming but may also promote changes in crystal structure and / or crystal imperfections.

#### 1.2.3.2 Effect on dissolution rate

The habit of a crystal can significantly influence its dissolution rate. This influence may be mediated through a change in the surface area to volume ratio of the crystal (in reference to the amount of surface area available for dissolution), through a change in the shape-related dissolution hydrodynamics and/or through possible anisotropy of the solid. Generally, changes in the habit of a material may produce changes in dissolution rate depending on both the nature of the rate-controlling step in the dissolution process and whether the crystals are isotropic or anisotropic (Burt and Mitchell, 1980). The former consideration refers to classification of the dissolution kinetics of the system as either transport controlled, surface reaction controlled or mixed transport-surface-controlled dissolution (see Section 1.4.1). If dissolution is transport controlled, the habit of the dissolving crystal will be of little significance. On the other hand, habit will play a decisive role when the surface reaction is rate determining. In those cases, the relative dissolution rates of the various crystallographic faces of the material become important. If the dissolution rate of all faces is the same, the crystal is said to be isotropic with respect to

dissolution. Otherwise, the crystal is said to be anisotropic. Burt and Mitchell (1979, 1980) have demonstrated dissolution anisotropy for the various habits of nickel sulfate crystals. There are several examples in the literature which illustrate the effect of habit on the bulk dissolution of a material. For example, Watanabe et al. (1982) observed significant differences in the dissolution rates of aspirin samples possessing differing crystal habits.

Both the significance and effect of flow hydrodynamics in a stirred system will depend on the flow conditions of the solvent (i.e., laminar or turbulent flow) and the rate determining step in the dissolution process (i.e., surface, transport or mixed control; see Section 1.4.1). A low fluid velocity characterized by a significant velocity component parallel to the surface and a very small flow velocity normal to the surface is typically known as laminar flow. A larger velocity which causes an abrupt change in the nature of the fluid flow in all directions signifies the existence of turbulent flow. In both cases, convection and diffusion both play a role in the transport of the solute material, with diffusive transport becoming most important in the region adjacent to the solid surface known as the diffusion layer (Levich, 1977). The nature and thickness of this layer will depend on the degree of agitation of the system as well as the characteristics of the solid surface such as the presence of corners / edges and the smoothness of the surface itself. Thus, a change in the shape of a solid could affect the nature of the diffusion layer thereby changing the flow of solvent over and near the surface, and ultimately, the dissolution rate of the solid (Levich, 1977).

The extent of the relationship between crystal habit and dissolution rate is still poorly understood however. This is due in part to the coexistence of other factors affecting the dissolution such as differences in crystal size, changes in crystal structure, and the presence of crystal imperfections (e.g., dislocations

and point defects) which tend to mask the contribution of crystal habit. The contributions of these factors must first be evaluated before the effect of habit on dissolution rate can be ascertained.

### 1.3 Crystal defects

Every crystal possesses some degree of structural imperfection which results in the disruption of the lattice and a change in the internal energy of the crystal. The extent (number) of these defects will depend on the history of the crystal including the conditions under which it was grown and the processes to which it has been subjected. Pharmaceutical scientists have often attributed changes in various physical properties of crystals to changes in the degree of imperfections although the mechanisms involved are not always well understood (e.g., Bundgaard, 1974; Jones, 1977; Hüttenrauch, 1978; Chiou and Kyle, 1979; Burt and Mitchell, 1981; Hull and Bacon, 1984). A better understanding of the effects of crystal defects would better allow researchers to exploit them in the formulation and manufacture of solid dosage forms.

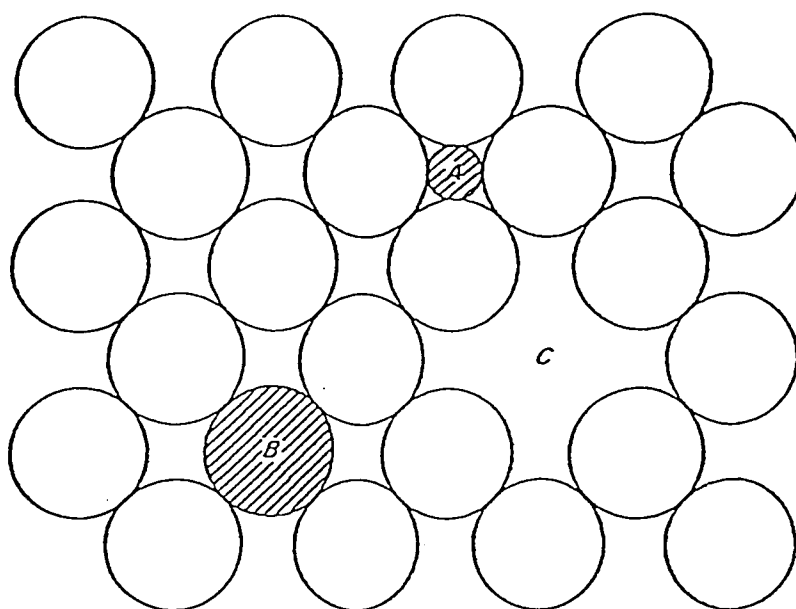
#### 1.3.1 Classification of crystal defects

Structural crystal defects may be categorized into point defects, line defects and plane defects.

##### 1.3.1.1 Point defects

Vacancy, interstitial (extra-atom) and substitutional defects are collectively known as point defects (Fig. 2). These defects are localized around a point and do not extend in any direction (i.e., they are zero dimensional).

Vacancies are voids caused by missing molecules, atoms or ions. These defects are common in ionic crystals, but, because the energy required to



- (A) Interstitial defect
- (B) Substitutional defect
- (C) Vacancy defect

Fig. 2 Three types of point defects (from Mullin, 1972).



create such a void in a molecular crystal (i.e., an organic crystal) can be quite substantial, vacancies are relatively rare in these crystals (Huttenrauch and Keiner, 1976). Interstitial defects occur when extra molecules, atoms or ions slip into the space between the regular lattice sites. These 'intruders' can be either of the same species as the rest of the crystal or a foreign species. Again, this type of defect is rarely seen in organic crystals where the interstitial spaces in the lattices are smaller than the sizes of most organic molecules, which thus prohibit their entrance due to the large lattice distortion that would result (Kitaigorodsky, 1973). Substitutional defects are caused by impurity molecules, atoms or ions occupying regular lattice sites. The probability of a substitutional defect occurring will be determined by the molecular volume of the impurity relative to that of the host (see Section 1.3.3).

#### 1.3.1.2 Line defects

Dislocations (or line defects) are one-dimensional defects and are generally divided into the following two categories: edge dislocations and screw dislocations. Edge dislocations (Fig. 3) are analogous to the insertion of an extra plane of molecules into a crystal lattice whereas screw dislocations (Fig. 4) are created when one section of the crystal shifts by one lattice spacing relative to the rest of the crystal resulting in a spiral formation around the dislocation line.

#### 1.3.1.3 Plane defects

Plane defects, or two-dimensional defects, include stacking faults which are caused by the irregular stacking of crystal planes (Fig. 5), and twinning which is the result of a process where two lattices of identical nature are combined in a composite crystal. These lattices may be in different orientations

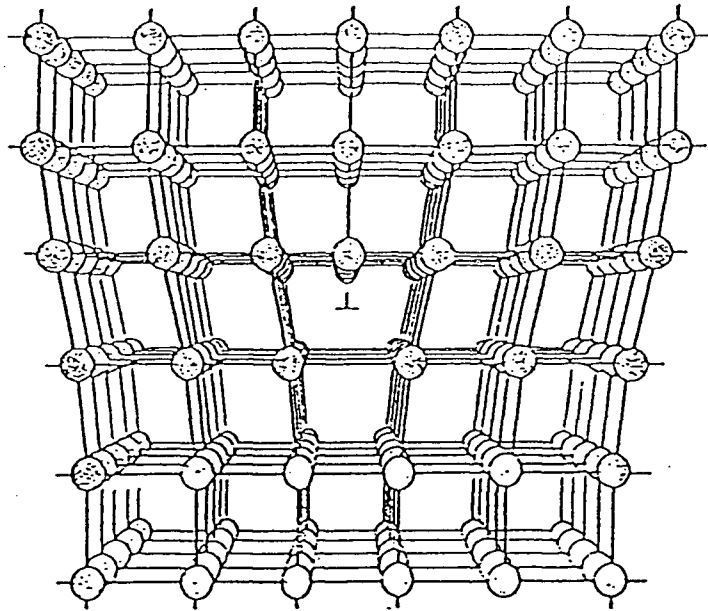


Fig. 3 An edge dislocation (from Moore, 1972).

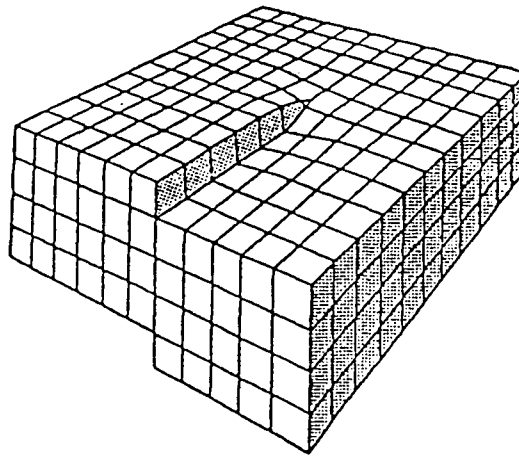


Fig. 4 A screw dislocation (from Mullin, 1972).

with respect to each other (Fig. 6). Since crystalline materials are often composed of a large number of small crystallites which are randomly oriented with respect to each other, another plane defect, the grain boundary, is formed where these crystallites meet (Fig. 7).

### 1.3.2 Formation of crystal defects

Defects may be introduced into crystals either during growth or during the processing and storage that ensues. Defects produced during growth may originate from one of the following (Klapper, 1979; Hull and Bacon, 1984): (a) continued growth of defects present in the seed crystals or other nuclei; (b) growth accidents such as interference from a different portion of the growing interface; (c) closure mistakes such as the inclusion of impurities; and (d) an accelerated growth rate which prevents the crystallizing molecules from attaining the proper orientation or enhances the probability of the inclusion of impurities (Klapper, 1979; Burt and Mitchell, 1981).

Defects may be generated following growth through the application of mechanical stresses such as grinding or milling, thermal stresses such as drying or even radiation stresses (Hull and Bacon, 1984). Huttenrauch and coworkers have extensively investigated the defects generated after growth and their potential applications in pharmaceutical processing (e.g., Huttenrauch, 1978). For example, Huttenrauch (1978) found that the progressive drying of lactose reduces its crystallinity (i.e., increases the degree of imperfections) proportionally and produces a more highly activated solid. This emphasizes that a simple process such as the drying of solids to remove residual water can also result in other significant structural changes such as increases in the degree of disorder in the solid.

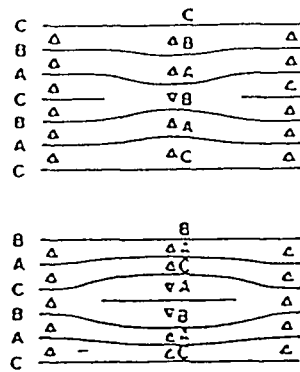


Fig. 5 A stacking fault (from Hull and Bacon, 1984).

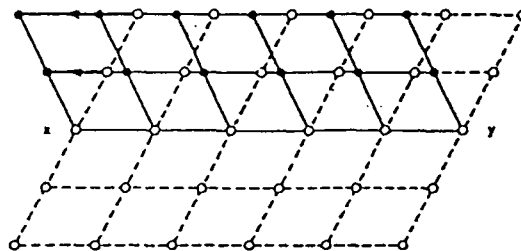


Fig. 6 A twinned structure where x-y is the trace of the twin composite plane (from Hull and Bacon, 1984).

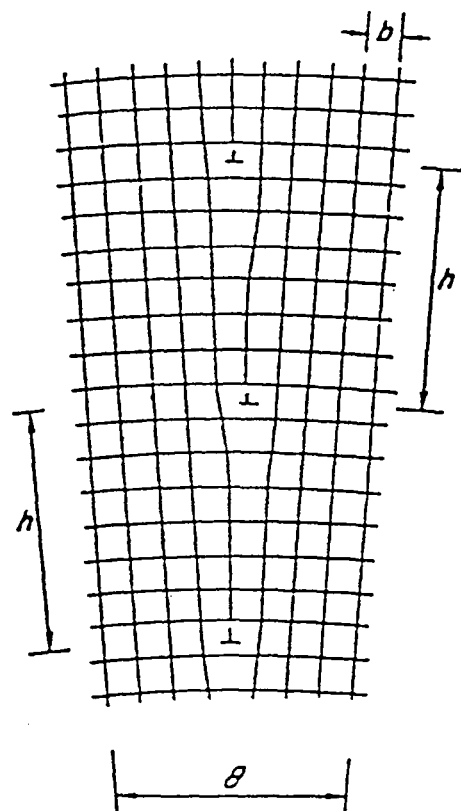


Fig. 7 A grain boundary (from Mullin, 1972).

### 1.3.3 Formation of impurity defects and solid solutions

Crystal defects can greatly affect the internal and surface energies of the solid in question. By creating regions of distortion and disruption in the lattice structure of a crystal, they can cause increases in the internal energy and entropy of the solid (York and Grant, 1985). The presence of impurity defects in the crystal can result in just such a situation.

Impurities can exist in the crystal lattice of a material at either a lattice site (i.e., a site normally occupied by a host species) or an interstice (i.e., a non-lattice position), resulting in the formation of either a substitutional or interstitial solid solution. As previously mentioned (Section 1.3.1.1), however, interstitial defects are rare in organic crystals due to steric hindrance.

#### 1.3.3.1 Substitutional solid solutions

Since electron transfer seldom occurs between molecules in organic crystals, favorable geometric factors tend to be the key and even decisive condition for solubility of an impurity in an organic solid (Kitaigorodsky, 1984). Under certain conditions, the degree of isomorphism i.e., the degree of similarity in shape and molecular volume between the impurity and the host molecules, will be not only a necessary but sufficient condition for the formation of solid solutions. The degree of isomorphism is determined by considering the coefficient of geometrical similarity ( $\epsilon$ ) of the two components. This is calculated by superimposing the molecules of the two components so as to maximize the intermolecular overlap followed by the application of Equation 8. The coefficient of geometrical similarity may be expressed as

$$\epsilon = 1 - T / r \quad (8)$$

where  $T$  refers to the volume of the non-overlapping parts and  $r$  is the volume of the overlapping parts of the two molecules. If the degree of geometrical similarity is significantly different from unity, then one can safely assume solubility is impossible (Kitaigorodsky, 1984). If the coefficient of geometrical similarity is greater than 0.85, it is likely that solubility is possible but it is not a certainty. One must then examine any changes in the molecular packing and intermolecular distances brought about by the presence of the impurity. If the protruding part of the impurity molecule i.e., the non-overlapping area, is located in a site where the packing is quite loose, then solubility may be possible. On the other hand, if the impurity site is in a tightly packed region the resulting distortion will make solubility unlikely if, upon substitution, the contraction of interatomic distances amounts to 10 - 15 % (Kitaigorodsky, 1984). It is also worth noting that an increase in density upon substitution is less tolerable than a decrease in density.

There are two important special cases where a satisfactory degree of isomorphism will not be sufficient to permit solubility of an impurity in a solid. First, if the impurity molecule breaks the hydrogen bonding network within the host solid, solubility will not occur. The gain in entropy can not compensate for the enthalpy gained through the breaking of the hydrogen bond. The second case arises when the dipole moments of the molecules can no longer compensate for each other. If a dipole moment is created, solubility will be restricted.

About two decades ago, Kitaigorodsky and coworkers came to the conclusion that there exists two types of substitutional solid solutions, namely, true and interblock substitutional solid solutions (Kitaigorodsky and Myasnikova, 1960). This categorization resulted from studies where incorporation of significant amounts of impurity (e.g., 3 %) into single crystals

was found to have no effect on the unit cell parameters of the crystals. In addition, geometrical analysis of optimum substitution in some of these instances (e.g., 1,8 - dinitronaphthalene in 1,5 - dinitronaphthalene) indicated that an increase in the unit cell parameters would be necessary in order to prevent unrealistic energy increases. These observations led Kitaigorodsky to suggest that there are two different mechanisms of substitution. When the impurity molecules replace the host molecules in the whole bulk of the crystal with a probability determined by concentration, a true substitutional solid solution is formed. This type of solution would produce changes in the dimensions of the average unit cell which could be detected by X-ray diffraction techniques. In the case of the interblock solid solution, the impurities occupy the defect sites of the crystal or are located at the boundaries of mosaic blocks. In these sites, the impurities have more room to adjust to the packing of the host. This type of solid solution can be identified when geometrical analysis of the substitution predicts a noticeable increase in the volume of the unit cell and experimentation finds otherwise.

#### 1.3.3.2 Energetics of solid solutions

The presence of additives or impurities in a crystal in the form of a solid solution (or molecular complex) is likely to significantly affect the overall energetics of the material with respect to the pure crystal form. In terms of impurity point defects alone, the change in the Gibbs free energy ( $\Delta G$ ) upon introducing each defect may be expressed by

$$\Delta G = G_{\text{cry}} - G_{\text{perf}} = \Delta H + kT [N \ln(N / (N + n)) + n \ln(n / (N + n))] - nT\Delta S \quad (9)$$



where  $G_{\text{cry}}$  and  $G_{\text{perf}}$  refer to the Gibbs free energies of the crystal under consideration and the hypothetical perfect crystal respectively,  $\Delta H$  and  $\Delta S$  are the enthalpy and entropy changes produced by the introduction of an impurity molecule,  $k$  is the Boltzmann constant,  $T$  is the absolute temperature,  $N$  is the number of host molecules and  $n$  is the number of impurity molecules in the crystal (Swalin, 1962). The central term in the right-hand side of Equation 9 represents the contribution made by the ideal entropy of mixing of the two components. Figure 8 illustrates the relative contributions of the enthalpy and entropy of the system and of the ideal entropy of mixing to the overall free energy change upon increasing the number of impurity defects present. At low concentrations of impurities, the contribution made by the ideal entropy of mixing dominates thus resulting in an overall decrease in the Gibbs free energy and a more stable crystal. As the concentration of defects increases, increases in lattice strain and in the vibrations of the molecules augments the enthalpy / entropy term more than the ideal entropy of mixing term. This results in an increase in the overall energy of the crystal making the resulting crystals less stable than those with fewer impurities. In summary, basic thermodynamics dictates that crystals containing a low number of impurity defects will be more stable than the pure crystals and those containing a large number of defects.

### 1.3.4 Pharmaceutical significance of crystal defects

#### 1.3.4.1 Effect on processing characteristics

Imperfections can have a profound effect on many of the mechanical properties of solids that are of interest in pharmaceutical manufacturing. For example, it has been found that the number of defects present in a powder can be correlated with the ease of deformation during compression (Hüttenrauch,

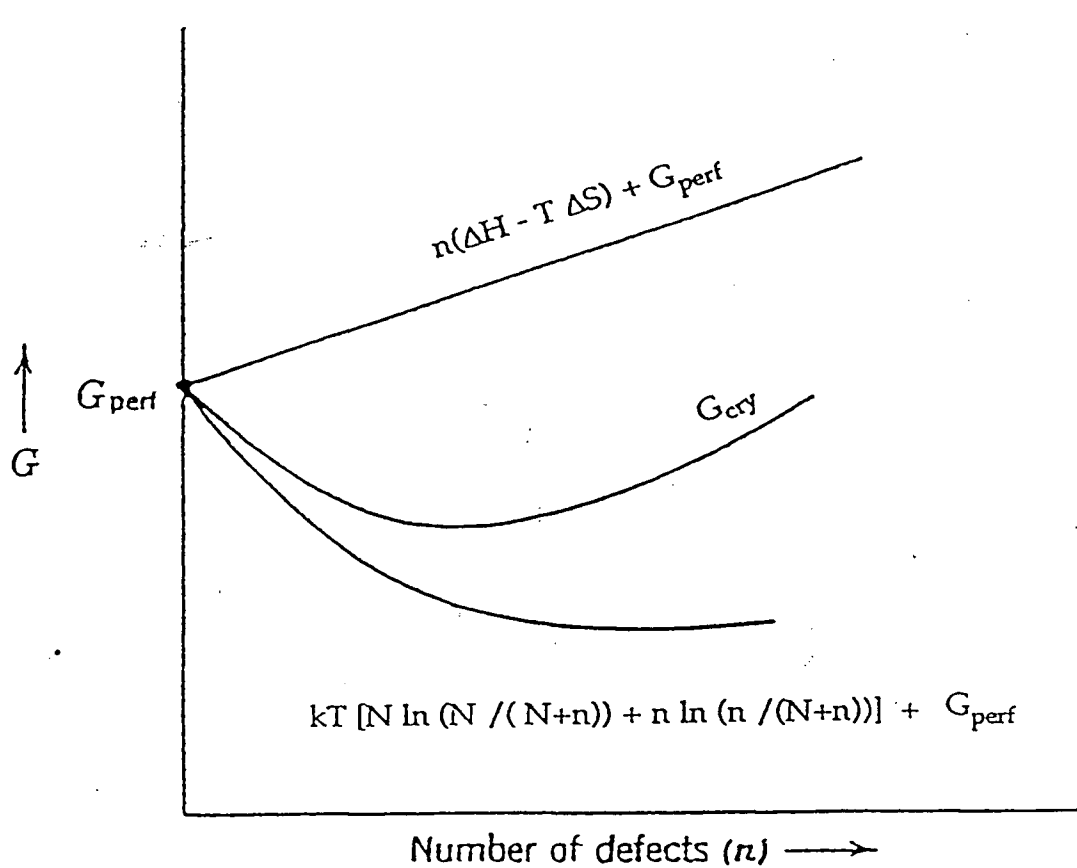


Fig. 8 Free energy of a crystal,  $G_{\text{cry}}$ , as a function of the number of impurity defects (middle line). The contribution of the change in enthalpy and entropy resulting from lattice defects is represented by the upper curve while the contribution of the ideal entropy of mixing is represented by the lower curve (modified from Swalin, 1962).

1977) and with the ease of fracture during compression or milling (Jones, 1977; Pilpel, 1977). The number of defects in a crystal can also increase or decrease the hardness of crystals. On one hand, defects make metals much more malleable than they would otherwise be (Hull and Bacon, 1984). On the other, by restricting molecular movements within the lattice, impurity defects can increase the strength of materials. For instance, mannitol - aspartame crystals are stronger than the pure mannitol (El-Shattway et al., 1984).

#### 1.3.4.2 Effect on stability

It is thought that most solid-state reactions begin at nuclei and defect sites (e.g., desolvation processes) (Byrn, 1982). Therefore, both the chemical and physical stability of a crystal may be affected by the number of defects it contains. A rather dramatic example of this phenomenon is the explosive nature of ammonium permanganate crystals grown from an aqueous solution by sudden cooling when exposed to a temperature of 78 °C. In comparison, the more well-formed crystals grown by isothermal evaporation are much more stable at the same temperature (Boldyrev et al., 1979). Another physically observable example of this phenomenon is the alpha / beta transition of *p*-dichlorobenzene. While 'perfect' alpha crystals do not transform, alpha crystals that have been pricked with a pin will react to produce the beta form of *p*-dichlorobenzene (Mnyukh et al., 1966).

#### 1.3.4.3 Effect on dissolution rate

It has been observed that the presence of crystal defects such as dislocations cause an increase in the energy and hence an increase in the dissolution rate of crystalline solids. Burt and Mitchell (1981) found that the density of dislocations in potassium perchlorate correlates with its dissolution

rate when the surface reaction plays a limiting role in the dissolution process. Furthermore, the alteration of the density of dislocations in digoxin by modification of crystallization conditions or by mechanical processing has been suggested to be a possible explanation for observed variations in the dissolution rate of the drug material in the dissolution rate of the drug material (Florence et al., 1974; Chiou and Kyle, 1979).

Impurity defects have also been demonstrated to play an important role in the dissolution process of a solid. Impurity defects may either increase or decrease the formation of active sites during the dissolution process. Bundgaard (1974) demonstrated that the incorporation of more than 0.25 % acetylsalicylic anhydride into acetylsalicylic acid crystals significantly lowers the dissolution rate of the crystals.

The presence of defects in crystals may account for variations in different batches of pharmaceutical materials. For example, the presence of defects may explain the variations observed in the dissolution rates of various aspirin samples (Mitchell et al., 1971; Jamali and Mitchell, 1973). A better understanding of the mechanisms by which crystal defects influence the dissolution rates of solids could lead to the exploitation of these mechanisms and to better quality control in pharmaceutical formulation and production.

#### 1.4 Dissolution of solids

As stated earlier, the diffusion-based theories of crystal growth originated with Noyes and Whitney (1897) who began with the premise that crystal growth may be considered to be the opposite of dissolution and that both processes are diffusion related. If this is true, then the dissolution process may be envisioned as one of solvation of solute material, potentially at defect sites on the solid surface (e.g., kinks), followed by movement along the surface and

finally transport away from the solid into the bulk of the solvent. Several approaches have been used to quantitate these processes as has also been adopted in the area of crystal growth (see Section 1.2.1). Perhaps the most valuable approach to understanding the dissolution process is the double barrier model which, as the name implies, involves both an interfacial barrier and a diffusion layer in its mechanistic description of dissolution (see Higuchi, 1967). The interfacial barrier describes the surface reaction through which the solute is liberated from the solid. This process is then followed by the transport of the solute away from the solid through the diffusion layer. Therefore, it can be assumed that the rate of dissolution will depend on the relative rates of these two steps with the slower of the two being the overall rate-determining step. Based on this, dissolution reactions are often divided into three categories as follows: a) transport controlled dissolution, b) surface reaction controlled dissolution, and c) mixed surface-reaction and transport-controlled dissolution (Wurster and Taylor, 1965a; Wurster and Taylor, 1965b; Higuchi, 1967; Mitchell and Saville, 1969).

#### 1.4.1 Kinetics of dissolution

##### 1.4.1.1 Transport-controlled dissolution

When the rate at which solute molecules are liberated into the interfacial layer that surrounds the dissolving solid is much greater than the rate at which they diffuse through the stationary boundary layer that separates the solid surface from the bulk of the dissolution medium, the dissolution process is said to be under transport control. In this instance, the rate of dissolution may be described by the Nernst - Brunner equation (Nernst, 1904; Brunner, 1905):

$$dm / dt = k_t A (C_s - C) \quad (10)$$

where  $dm / dt$  represents the rate of transport,  $k_t$  is the coefficient of transport,  $A$  is the surface area of the solid,  $C_s$  is the concentration of the saturated solution (i.e., the concentration in the interfacial layer) and  $C$  is the concentration in the bulk of the solution. The coefficient of transport,  $k_t$ , is given by Equation 2 which indicates that the transport coefficient, and hence, the rate of dissolution, is inversely proportional to the thickness of the diffusion layer ( $h$ ). In turn, since  $h$  is typically defined as the average distance from the surface of the solid to the point at which the effects of the agitation become significant, the degree of agitation will determine the rate of dissolution.

#### 1.4.1.2 Surface-reaction controlled dissolution

The rate of dissolution will not always be controlled by the rate of diffusion. For example, if the degree of agitation in the system is sufficiently large to make the thickness of the diffusion layer very small, the solute molecules may be transported away from the interface faster than they can be replaced by liberation from the surface. In this case, as in instances where the solid is very insoluble, the rate of dissolution is controlled by the surface reaction process. The rate of dissolution of surface-reaction controlled processes may be described by

$$dm / dt = k_r A (C_s - C)^n \quad (11)$$

where  $k_r$  is the rate constant for the surface reaction and  $n$  is some positive integer that represents the order of the reaction.

When the dissolution process is surface-controlled, the rate of dissolution becomes a function of the energetics of the surface reaction. Under such conditions, the energy required to remove a solute molecule from the surface of the solid, the energy of solvation and the energy required to initiate diffusion (i.e., the activation energy) all influence the rate of dissolution.

#### 1.4.1.3 Mixed surface-reaction and transport-controlled dissolution

When  $k_t$  and  $k_r$  are similar in magnitude, factors affecting either the transport process or the surface reaction will influence the rate of dissolution of the solid material. In such an instance, the dissolution process is said to be under mixed surface and transport control and may be described by

$$dm / dt = k_{obs} A (C_s - C) \quad (12)$$

where  $k_{obs}$  is the observed rate constant for the mixed control dissolution process. The observed rate constant,  $k_{obs}$ , can be expressed in terms of the rate constants for transport control and surface control as follows (Bircumshaw and Riddiford, 1952):

$$k_{obs} = k_t k_r / (k_t + k_r). \quad (13)$$

In this instance, both the degree of agitation and the energetics of the surface reaction will play an important role in establishing the overall rate of dissolution.

#### 1.4.2 Factors affecting dissolution

The influence of crystal habit and crystal defects on dissolution has already been discussed in Sections 1.2.3.2 and 1.3.4.3. Other factors of

importance include degree of agitation, temperature, solubility, concentration gradient and composition of the dissolution medium (Bircumshaw and Riddiford, 1952; Wurster and Taylor, 1965). As has been discussed above, the degree of agitation plays an important role in the transport controlled dissolution process in that it directly determines the thickness of the diffusion layer. The temperature at which dissolution occurs also has an important bearing on the observed rate of dissolution for both transport and surface reaction controlled systems although perhaps more so in the case of the surface-reaction controlled process (Bircumshaw and Riddiford, 1952). An increase in temperature brings about increases in the energy of both the surface reaction and the transport process, as demonstrated by increases in the respective rate constants (i.e.,  $k_r$  and  $k_t$ ) (Wurster and Taylor, 1965). The solubility of the solute plays a role in that it is directly involved in the concentration gradient, the  $(C_s - C)$  term of Equations 10, 11 and 12, which represents the driving force for the dissolution process. In order to maximize the rate of dissolution, it is important to maintain sink conditions, which become operative when the concentration of solute in the bulk of the solution ( $C$ ) is no more than 10 -20 % of the solubility ( $C_s$ ) (Gibaldi and Feldman, 1967). The nature and composition of the dissolution medium is also an important consideration. Variables such as pH (important for acidic or basic materials), viscosity (important for transport controlled processes), polarity and the presence of solubilizing additives will all contribute to the final observed rate of dissolution.

### 1.5 Phenytoin as a model

Previous studies have demonstrated that several pharmaceutically important properties of acetaminophen, a common analgesic and antipyretic, can be reproducibly modified by crystallizing the drug from solutions containing



various concentrations of the additive, *p*-acetoxycetanilide, which is both a synthetic impurity and a suggested prodrug of acetaminophen (Chow et al., 1985). Properties such as the habit, size, density, fusion energetics and intrinsic dissolution rate of acetaminophen were all affected by the incorporation of the additive. However, X-ray diffraction studies did not detect any changes in the diffraction pattern of the drug indicating that gross crystalline changes did not occur. Chow et al. (1985) attributed the changes in the physical and thermal properties of the drug to changes in the nature and extent of crystal imperfections, and the changes in dissolution rate to an interplay between the following factors: (1) crystal anisotropy; (2) hydrodynamics during dissolution; (3) crystal imperfections; and (4) non-stoichiometric hydrates. These results led Chow et al. (1985) to suggest not only that traces of non-toxic additives may provide a means of controlling crystal energy, crystal order, water content, dissolution rate and possibly bioavailability, but also that the presence of impurities may account for certain batch-to-batch variations in the properties of solid drugs and excipients. To evaluate both the universality and utility of such an approach to crystal engineering, studies similar to those performed with acetaminophen have been extended to another problematic drug, phenytoin.

Phenytoin (5,5-diphenylhydantoin; DPH) (Fig. 9) is an anticonvulsant agent that has been commonly used in the treatment of grand mal epileptic seizures since its introduction in 1938 (Merritt and Putnam, 1938). The popularity of phenytoin as an antiepileptic agent may be attributed to its effective anticonvulsant action coupled with an absence of the hypnotic action which is commonly observed with barbituates. DPH is subject to poor and / or erratic absorption in various dosage forms, whether present as the free acid or the sodium salt (Rail, 1968; Arnold et al., 1970; Suzuki et al., 1970; Stella et al.,

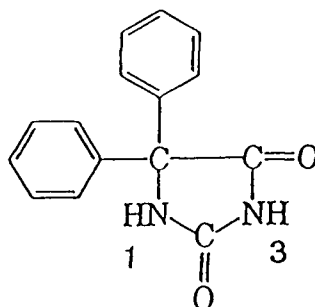
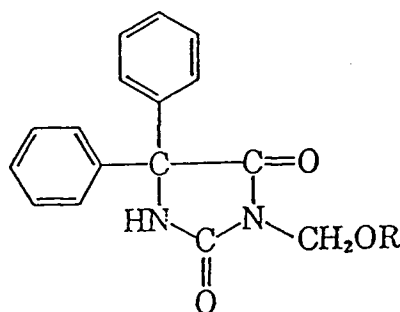


Fig. 9 Chemical structure of phenytoin (5,5-diphenylhydantoin; DPH).



	R
II	H-
III	CH <sub>3</sub> CO-
IV	C <sub>2</sub> H <sub>5</sub> CO-
V	COCH <sub>2</sub> N <sup>+</sup> H(CH <sub>3</sub> ) <sub>2</sub> CH <sub>3</sub> SO <sub>3</sub> <sup>-</sup>
VI	PO <sub>3</sub> <sup>2-</sup> Na <sub>2</sub> <sup>+</sup>

Fig. 10 Chemical structures of (II) 3-hydroxymethyl-5,5-diphenylhydantoin, (III) 3-acetoxymethyl-5,5-diphenylhydantoin, (IV) 3-propanoyloxymethyl-5,5-diphenylhydantoin, (V) 3-hydroxymethyl-5,5-diphenylhydantoin N,N-dimethylglycine ester methanesulfonate and (VI) 3-hydroxymethyl-5,5-diphenylhydantoin disodium phosphate ester.

1975). This problem may be related to phenytoin's low aqueous solubility and dissolution rate as well as its relatively high  $pK_a$  (8.3).

Single crystal X-ray diffraction studies indicate that DPH crystallizes in the orthorhombic system in the space group  $Pn2_1a$  (cell dimensions  $a = 6.230$ ,  $b = 13.581$ ,  $c = 15.532$  Å,  $Z = 4$ ) (Camerman and Camerman, 1971). Chakrabarti et al. (1978) have suggested that DPH may also exist in the form of a second polymorph (Form II) or solvate. Nonetheless, the orthorhombic form is the most commonly observed and most stable arrangement for DPH. Structural analysis indicates that the DPH molecules in the crystal lattice are involved in an extensive intermolecular hydrogen bonding network with the hydrogens bonded to the nitrogen atoms attached to the two carbonyl oxygen atoms. The strength of this interaction is demonstrated by the short H....O hydrogen bond distances of 1.92 Å (H (1)....O (7')) and 1.98 Å (H (3)....O (6')) (Camerman and Camerman, 1971). This extensive network of hydrogen bonds bestows upon phenytoin a strong crystal lattice which is reflected in its high melting point of 295 °C (Philip et al., 1984). Consequently, DPH's sparing solubility may be ascribed to the strength of its crystal lattice. These factors suggest that if the lattice of DPH were 'weakened', perhaps by the incorporation of additives, there could be corresponding changes to the solubility and dissolution rate of the material.

## 1.6 Crystal modification of phenytoin

Various techniques have been used to modify DPH crystals in an attempt to develop a more bioavailable and more uniform dosage form. It has been found that solid dispersions of DPH with water soluble carriers such as polyethylene glycol (PEG) (Chiou, 1977; Yakou et al., 1984; Jachowicz, 1987),

polyvinylpyrrolidone (PVP) (Jachowicz, 1987) and urea (Jachowicz, 1987) result in substantially higher rates of dissolution of DPH than those observed with the pure material. Along a similar line, coprecipitation of DPH with materials such as PVP (Sekikawa et al., 1978; Yakou, 1986), PEG (Yakou, 1986), sodium deoxycholate (Yakou, 1986) and hydroxypropylcellulose (Yakou, 1986) has been found to produce a significant improvement in the dissolution rate of DPH. Other investigations have pursued the complexation of DPH with inert materials such as cyclodextrins (Frank, 1975; Jones et al., 1984a, 1984b; Menard et al., 1988) and polymers of cyclodextrin and epichlorohydrin (Uekama, 1985). These studies have also demonstrated a significant enhancement in the solubility and dissolution rate of DPH. However, since these solid modifications of DPH are highly energetic and thus, are thermodynamically unstable, they will revert to the more stable form, which would nullify the intended improvement in solubility and bioavailability of the material.

#### 1.6.1 Methyl ester prodrugs of DPH

In an effort to address DPH's problem of erratic bioavailability, Stella and co-workers have investigated the possibility of improving DPH's bioavailability through the development of low-melting prodrugs that could be incorporated into metabolizable vehicles suitable for formulation in soft gelatin capsules or for microencapsulation (Yamaoka et al., 1983; Varia et al., 1984a). Based on the hypothesis that substitution for the hydrogen atom on N (3) (fig. 10) would disrupt DPH's hydrogen bonding pattern in a bioreversible fashion (Yamaoka et al., 1983), 3-hydroxymethyl-5,5-diphenylhydantoin (HMDPH) and various straight chain acyl derivatives of HMDPH were prepared. Studies on these derivatives led Yamaoka et al. (1983) to conclude the following: (1) that

these DPH derivatives are more readily soluble in various metabolizable glycerol esters (e.g., tributyrin, triolein) than DPH; (2) that the solubilities of the proposed prodrugs in the various organic solvents studied (e.g., cyclohexane, ethyl oleate, triolein) showed a strong correlation with the melting points of the material; and (3) that 3-pentanoyloxymethyl-5,5-diphenylhydantoin administered in tributyrin gave superior oral DPH bioavailability in rats when compared with sodium phenytoin administered as an aqueous solution. Yamaoka et al. (1983) also found that the acyl methyl ester derivatives of DPH reverts to the parent DPH molecule via cleavage of the ester bond followed by a rapid dehydroxymethylation step to generate DPH and formaldehyde.

Further studies with methyl esters containing ionizable groups in the ester moiety have indicated that an amino acyl ester, 3-hydroxymethyl-5,5-diphenylhydantoin N,N-dimethylglycine ester methanesulfonate (Fig. 10) may be useful as a prodrug for oral administration while 3-hydroxymethyl-5,5-diphenylhydantoin disodium phosphate ester (Fig. 10) may be suitable for parenteral administration (Varia et al., 1984a; Varia et al., 1984b; Varia and Stella, 1984a). In vivo studies in rats and dogs have suggested that these prodrugs should be further assessed for their potential utility in DPH's therapy (Varia and Stella, 1984a; Varia and Stella, 1984b).

### 1.7 Scope of study

In light of the results obtained in crystal engineering studies using acetaminophen (Section 1.5; Chow et al., 1985) and the possible utility in disrupting the hydrogen bond network of DPH (see Section 1.6.1), the work presented in this thesis is based on the hypothesis that incorporation of traces of a chemically related additive into DPH crystals will produce a significant modulation of their physicochemical properties, dissolution rate and potentially,

their bioavailability. This thesis describes the synthesis of a potential prodrug of DPH (Varia et al., 1984a), 3-propanoyloxymethyl-5,5-diphenylhydantoin (PMDPH) (Fig. 10), the crystallization of DPH in the presence of various concentrations of this additive and the characterization of the resulting crystal samples. The DPH samples were characterized in terms of crystal structure, crystal habit, size, surface area, additive sorption, fusion energetics and dissolution rate.

The results of these investigations are discussed with reference to those obtained from similar studies in our laboratory employing 3-acetoxymethyl-5,5-diphenylhydantoin (AMDPH) (Fig. 10) as the crystallization additive. AMDPH, also cited as a potential prodrug of DPH (Varia et al., 1984) differs from PMDPH in that its ester side chain is shorter by one methylene group.

The specific objectives of the present work were as follows:

- 1) To synthesize 3-propanoyloxymethyl-5,5-diphenylhydantoin (PMDPH), to be used as a crystallization additive.
- 2) To crystallize DPH under controlled conditions in the presence of various concentrations of PMDPH.
- 3) To examine and characterize the physical properties of these crystals.
- 4) To compare the results with those obtained in studies with AMDPH.
- 5) To establish some general guidelines for the selection of homologous crystallization additives for doping drug crystals.

## 2. EXPERIMENTAL

### 2.1 Materials

Acetone, BDH Chemicals

Argon / methane (95:5), Matheson Gas Products Canada

Cyclohexanone, Sigma Chemical Co.

1-Bromobutane, Matheson, Coleman and Bell Manufacturing Chemists

1-Butanol, BDH Chemicals

Diethyl ether, BDH Chemicals

Dimethyl sulfoxide (d6), Aldrich Chemical Co.

5,5-Diphenylhydantoin, Sigma Chemical Co.

Ethanol, Stanchem

Formaldehyde solution (37-41 % v/v formaldehyde; Formalin), BDH Chemicals

Helium, Matheson Gas Products Canada

Hydrogen (ultra pure), Matheson Gas Products Canada

Hydrochloric acid, BDH Chemicals

Indium, Calibration Sample Kit, Perkin Elmer Corporation

Isopropanol, BDH Chemicals

Krypton in helium gas: 0.0322 and 0.1093 % Kr Matheson Gas Products  
Canada, 0.075 % Kr Linde Union Carbide

Medical air, Linde Union Carbide

Methanol, BDH Chemicals and Caledon Chemical Co. (for GC analysis)

Nitrogen (ultra-pure), Linde Union Carbide

Potassium Carbonate, BDH Chemicals

Potassium dihydrogen orthophosphate, BDH Chemicals

Propionic anhydride, BDH Chemicals

Sulfuric acid, BDH Chemicals

Tetrahydrofuran, BDH Chemicals

Toluene, BDH Chemicals

Water, deionized via a Milli-RO Water System , Millipore Corp.



## 2.2 Equipment

Balances, models PJ300 and AJ100 from Mettler Corp.

Differential scanning calorimeter, Model 910 with a thermal analyzer

(Series 99), DuPont Instruments

Dissolution-testing apparatus: Vanderkamp 600 Six-spindle dissolution tester,

Vanderkamp Fraction collector Model 10 and Vanderkamp

Programmable dissolution sequencer EDS-10, VanKel Corp.

Gas chromatograph, Hewlett Packard model 5840A with Hewlett Packard

7671A Auto Sampler, 18835B Capillary Inlet System and Ultra 2

(Crosslinked 5% phenylmethylsilicone) 50m X 0.32  $\mu$ m film thickness

capillary column. The injection port consists of a narrow base glass inlet

packed with silanized glass wool.

Gastight syringe model 1710 (0.1 mL), Hamilton Co.

High performance liquid chromatograph: Series 1050 HPLC pump,

Series 1050 variable UV detector and Model 3396A integrator, Hewlett

Packard Co., Micropore ODS-Hypersil column (2.1 X 100 mm), Hewlett

Packard Co.

Hot plate/stirrer, Corning model PC-351 and Fisher Thermamix

Nuclear magnetic resonance (NMR) spectrometer, Bruker WH-400 (400 Mz)

Particle size analyzer, Brinkman model 2010, interfaced with IBM ps/2

computer

Pipettes, variable volume, Gilson Co. and Eppendorf Co.

Scanning Electron Microscope, Hitachi S-570

Stirrers, variable speed paddle, Heidolph Co. model RZR-2000

Surface area analyzer, Quantasorb, Quantachrome Corp.

Temperature regulators for water baths, Julabo Co. model P and Haake E8

Ultraviolet / visible diode array spectrophotometer, Hewlett Packard Co., model 8452A

Water baths: Circulating water bath, Techne C-400 and  
sonicating water bath, Branson 2200

X-ray diffractometer, Rigaku Geigerflex interfaced with an IBM compatible pc  
through a data processing computer unit (D/Max-B Control)

## 2.3 Preparation and characterization of 3-propanoyloxymethyl-5,5-diphenylhydantoin (PMDPH)

### 2.3.1 Synthesis of PMDPH

The synthetic intermediate, 3-hydroxymethyl-5,5-diphenylhydantoin (HMDPH), and the product, PMDPH, were prepared according to the methods described by Varia et al. (1984) with modifications. DPH (40 g) was suspended in a solution of potassium carbonate (11.4 g) in distilled water (1.44 L). A 37 - 41 % formalin solution (160 mL) was slowly added to this suspension and the resulting mixture stirred overnight using a magnetic bar at room temperature. The resulting solid mixture of DPH and HMDPH was filtered and allowed to air-dry for 48 hours yielding 37g of solid mixture (60 - 80 % HMDPH). The dried solid mixture (37 g) was suspended in an excess of propionic anhydride (140 mL) with the aid of stirring. Concentrated sulfuric acid (0.4 mL) was added to the suspension which was continuously stirred for another 10 - 15 minutes. The reaction mixture was then diluted with diethyl ether (~ 100 mL) after which the solid was filtered, washed with diethyl ether (100 mL) and recrystallized twice from ethanol. (It was found to be necessary to dilute the reaction mixture with diethyl ether before filtration of the solid in order to protect the filter paper from the corrosive effects of the propionic anhydride.) The final yield was 31.5 g of PMDPH.

### 2.3.2 Characterization of PMDPH

The synthetic product was characterized by differential scanning calorimetry and solution  $^1\text{H}$ -nuclear magnetic resonance (nmr) spectroscopy.

#### 2.3.2.1 Differential scanning calorimetry

The melting point of PMDPH (0.002 - 0.003 g) was determined by differential scanning calorimetry in hermetically sealed aluminum pans heated at a rate of 10 °C / min. The melting point was taken as the temperature at the point of intersection of the leading line of the steepest slope and the baseline.

#### 2.3.2.2 Solution $^1\text{H}$ -nmr spectroscopy

The  $^1\text{H}$ -nmr spectrum of PMDPH (0.02 - 0.03 g) was determined using d6-dimethyl sulfoxide (d6-DMSO) as the sample solvent and tetramethylsilane (TMS) as an external reference. Since d6-DMSO is extremely hygroscopic, the sealed ampoule containing the solvent was opened just before adding the solvent to the sample. After opening the ampoule, 2 -3 mL of the solvent was quickly transferred to an nmr tube containing the solid sample. The tube was then immediately sealed with a cap and a piece of parafilm. As a result of taking these precautions, the nmr spectra of these samples contained relatively small peaks due to the presence of water (Fig. 11).

#### 2.4 Batch crystallization of DPH from methanol

DPH (13 g) and PMDPH ( $0\text{--}11\text{ g L}^{-1}$ ) were dissolved in 400 mL (316.4 g) of methanol in a 500 mL erylenmeyer flask under mild reflux. Following equilibration at 50° C for 30 minutes in a sealed flask, the solution was quickly transferred to a 500 mL three-necked, round bottomed flask immersed in a thermostatic water bath maintained at  $30 \pm 0.5$  °C. The solution was seeded with 1-2 mg of DPH crystals ( $< 75\text{ }\mu\text{m}$ ), and stirred at  $250 \pm 1$  rpm for two hours. These conditions correspond to an initial supersaturation of  $6.5\text{ g kg}^{-1}$  at 30°C. The crystals were then filtered by means of suction, air-dried for two days and stored in a desiccator under vacuum.

## 2.5 Determination of sorption of PMDPH by DPH crystals

The amount of PMDPH sorbed by the DPH crystals was determined by high performance liquid chromatography (HPLC) using a Hewlett Packard 1050 liquid chromatograph, a Hewlett Packard 1050 variable wavelength UV detector and a mobile phase consisting of 52% 0.003 M  $\text{KH}_2\text{PO}_4$  buffer / 48 % methanol at a flow rate of 0.5 mL/min. Toluene was used as the internal standard and methanol as the sample solvent. A calibration curve for PMDPH was obtained at a UV detection wavelength of 230 nm using solutions of varying amounts of PMDPH (4 - 20  $\mu\text{g}$ ) and a constant amount of toluene (100  $\mu\text{L}$  of a 3 % v/v toluene in methanol stock solution). For the analysis, the crystals (20 - 30 mg) were dissolved in a few millilitres of methanol in a 10 mL volumetric flask to which 100  $\mu\text{L}$  of the toluene solution was added previous to making up to final volume with methanol. Five  $\mu\text{L}$  samples were injected.

## 2.6 Surface-adsorbed additive determination

HPLC utilizing the same analytical conditions as those described above was used to determine the amount of additive adsorbed on to the surface of the DPH crystals. The crystals (0.020 g) grown in the presence of 3, 5 and 7  $\text{g L}^{-1}$  PMDPH were repeatedly washed by vortex mixing with four 2 mL aliquots of 5 % methanol in water for 2 minutes each. The supernatant of each wash was filtered through a Millipore filter. For the analysis, 50  $\mu\text{L}$  of toluene solution (see Section 2.5) was mixed with 0.9 mL of the filtrate. Ten  $\mu\text{L}$  samples were analyzed for both DPH and PMDPH content.

## 2.7 Determination of residual methanol content in DPH crystals

### 2.7.1 Assay procedure

The amount of residual methanol present in the DPH crystals was determined by gas chromatography (GC) utilizing a Hewlett Packard 5840A chromatograph as described in Section 2.2 and the operating conditions described below (section 2.7.2). Cyclohexanone was used as the sample solvent and isopropanol as the internal standard. A standard curve was determined employing samples containing 0.01 - 0.4 mL of a methanol (100 ppm) in cyclohexanone stock solution and 0.1 mL of an isopropanol (50 ppm) in cyclohexanone stock solution diluted to a total volume of 1 mL with cyclohexanone (i.e., final concentrations of 1 - 40 ppm methanol, 5 ppm isopropanol). DPH crystals (0.05 g) were dissolved in cyclohexanone mixed with 0.1 mL of the isopropanol stock solution and diluted to a total volume of 1 mL with cyclohexanone. Two  $\mu$ L samples were injected with a split ratio of 30:1.

#### 2.7.2 Gas chromatographic conditions

The GC operating conditions were as follows: injection temperature 160 °C; initial column temperature 60 °C for 4.2 min, followed by an increase at a rate of 30 °C / min to a temperature of 130 °C; detector (FID) temperature 250 °C; carrier gas (helium UHP) flow 1 mL / min; hydrogen UHP flow 30 mL / min; air flow 240 mL / min; auxiliary gas (helium) flow 30 mL / min; head pressure 7 p.s.i.; chart speed 1 cm / min; slope sensitivity 0.03; area rejection 1; attenuation 2<sup>3</sup>.

#### 2.8 Powder X-ray diffraction

Powder X-ray diffraction studies were performed on the DPH crystals using Cu K $\alpha$  X-rays with a nickel filter on a Rigaku Geigerflex powder X-ray diffractometer. The sample (0.05 g) was packed in a glass sample holder using

a glass microscope slide, and then scanned from  $2\theta = 5$  to  $55^\circ$  at a speed of  $5^\circ$  / min.

## 2.9 Scanning electron microscopy

A thin coat of graphite glue was applied to the face of a metal stub (sample holder) with a small paint brush. When the glue had almost dried (after 10 - 20 seconds), a small quantity of DPH sample crystals were sprinkled onto the stub. The excess or unattached crystals were then shaken off the face of the stub. The adhered crystals were then coated with gold under vacuum. The habits and surface features of the crystals were examined at various magnifications using a Hitachi S-570 scanning electron microscope.

## 2.10 Particle size distribution

The particle size distribution of the DPH samples was examined using a Brinkman laser-based optical particle size analyzer equipped with a charge coupled device microscopic video camera for image analysis. The crystals (0.05g) were suspended in 2 mL of 1-bromobutane in a quartz cell equipped with a magnetic stirrer. The specific lengths and widths of crystals were determined from particle images 'frozen' by a pulsed light (strobe) technique and 'captured' by an IBM computer equipped with specialized software. The specific length and width were calculated as follows:

$$\text{Specific length} = (\text{perimeter} + \sqrt{\text{perimeter}^2 - \text{area} \times 16}) / 4 \quad (14)$$

$$\text{Specific width} = (\text{perimeter} - \sqrt{\text{perimeter}^2 - \text{area} \times 16}) / 4 \quad (15)$$

## 2.11 Specific surface area measurements

The specific surface area of the DPH crystals was determined using a B.E.T. triple-point gas adsorption technique with 0.0322, 0.075 and 0.1093 %

krypton in helium as adsorbate. DPH crystals (0.2 - 0.4 g) were packed into a glass sample holder until the holder's reservoir was about three quarters full. (It is important to leave an unobstructed path for gas flow through the reservoir above the solid material.) The sample holder was then attached to a Quantasorb surface area analyzer in such a way that the arm down which the sample had been loaded acted as the inlet for the gases into the holder. This step is to ensure that any crystals which remained adhered to the side of the holder arm would be pushed into the main reservoir by the gas flow and not out of the holder and into the equipment itself. The samples were outgassed by repeated adsorption (at 77 K, using liquid nitrogen) and desorption (at 295 K) of krypton until a constant desorption peak was attained. Each measurement was calibrated by injecting a volume of pure nitrogen equivalent to within  $\pm 10\%$  of the volume of krypton adsorbed.

The specific surface area,  $S$ , was calculated using the BET isotherm as follows (Lowell, 1979):

$$1 / [w (P_o / P - 1)] = (C - 1) / w_m C (P / P_o) + 1 / w_m C \quad (16)$$

where  $w$  and  $w_m$  are the total weight of krypton adsorbed and the weight of a hypothetical monolayer at a relative pressure  $P / P_o$  respectively, while  $P$  and  $P_o$  are the partial pressure and the saturated vapor pressure of the adsorbate.  $C$  is a constant which is directly related to the enthalpy of adsorption for the system. Based on Equation 16, a plot of  $1 / [w (P_o / P - 1)]$  versus  $P / P_o$  will be linear with:

$$\text{slope} = (C - 1) / w_m C \quad (17)$$

$$\text{and intercept} = 1 / w_m C \quad (18)$$



S may then be calculated from the following equation:

$$S = w_m N a / M w_s \quad (19)$$

where N is the Avagadro constant, a is the effective cross-sectional area of the adsorbed molecule (20.5 Å for krypton), a is the effective cross-sectional area of the adsorbed molecule (20.5 Å<sup>2</sup> for krypton), M is the molecular weight of the adsorbate and w<sub>s</sub> is the sample weight. The surface area calculations were performed on an IBM compatible computer using a program written in BASIC.

## 2.12 Differential scanning calorimetry

The enthalpy of fusion,  $\Delta H^f$ , and melting point, T<sub>m</sub>, of the DPH samples (2-3 mg) were determined in hermetically sealed aluminum pans heated at a rate of 10 °C /min over the range of 30° - 320 °C, using nitrogen as the purge gas and indium (5.96, 8.43, 14.76 and 18.57 mg samples) as the calorimetric standard. The melting point was taken as the temperature at the point of intersection of the leading line of the steepest slope and the base line. The enthalpy of fusion was calculated from the peak area which was determined using an integration routine on an Apple II plus computer interfaced with a Dupont (Series 99) thermal analyzer.

## 2.13 Solubility of PMDPH-doped DPH crystals in water

DPH crystals (0.01 g) grown in the presence of 0, 4 and 7 gL<sup>-1</sup> were placed in 15 mL test tubes equipped with teflon coated screw caps. Following the addition of one mL of distilled water, the tubes were vortexed and placed in a shaking water bath at 30 °C until equilibrium was reached (about 15 days).

The samples were prepared for HPLC analysis by placing 0.6 mL of supernatant, which had been filtered through glass wool, in a 10 mL volumetric flask along with 25  $\mu$ L of the internal standard solution (a 2 mg / mL solution of benzophenone in methanol) and brought up to volume with methanol. A calibration curve for DPH was determined by analyzing solutions containing varying concentrations of DPH (1.1 - 3.3  $\mu$ g / mL) and a constant amount of benzophenone (5  $\mu$ g / mL). The HPLC conditions used were identical to those described in Section 2.5. 15  $\mu$ L samples were injected.

#### 2.14 Dissolution studies

The dissolution profile of DPH crystals (0.02 g) was determined in water at 25° or 37 °C using an automated six-spindle dissolution tester (Vanderkamp system, VanKel) and the USP/NF XVI (1985) dissolution Method 2 with paddle stirring at 50 - 250 rpm (at 25 °C) and at 100 rpm (at 37°C). The dissolution medium consisted of 900 mL of degassed distilled water containing hydrochloric acid (0.001 M) and Brij 30 (1 in 112,500 v/v). Samples were withdrawn by an automated sample collector (Vanderkamp EDS-10) at 5, 10, 15, 30, 60 , 90, 120, 300 and 720 minutes after the addition of the samples to the dissolution medium. The samples were analyzed for DPH by UV spectrophotometry at 230 nm using a diode array spectrophotometer. A calibration curve was prepared using a series of solutions containing varying amounts of DPH (1 - 17 mg DPH / mL of dissolution medium).

### 3. RESULTS AND DISCUSSION

#### 3.1 Preparation of PMDPH

##### 3.1.1 Synthesis

Attempts to synthesize HMDPH following the procedure detailed by Varia et al. (1984) resulted in an unacceptably low percentage yield of the product (~20%). In order to raise the product yield, the procedure was modified to increase significantly the amount of base available for the reaction (see Section 2.3.1). The resulting yield was 60 - 80 %. While the yield was still less than optimal, the simplicity of the procedure favoured its use over the alternatives which involve the use of an organic base and solvent. Preliminary trials with one of these alternatives utilizing paraformaldehyde, diisopropylamine and DPH in tetrahydrofuran, also produced a relatively high HMDPH yield (~80 %). However, the protocol involved both rotary evaporation as well as an extensive washing of the product making it less attractive than the modified method of Varia et al. (1984).

The similarities in the structures of HMDPH and DPH made the purification of HMDPH difficult without incurring significant loss of the product itself. Thus, the crude product was used without further purification in the subsequent synthesis of PMDPH. The method was based on that described by Varia et al. (1984) for the preparation of AMDPH. The final product, which was determined to be primarily PMDPH (see Section 3.1.2), was recrystallized twice from ethanol to produce a white solid of at least 99 % purity as determined by HPLC. The DPH carried over from the preparation of HMDPH appeared to have remained dissolved in the large excess of propionic anhydride used in the final step. Yamaoka et al. (1983) described a basic protocol for the preparation

of the homologous series of methyl esters of DPH including AMDPH and PMDPH. This procedure involves the use of the corresponding acid chloride with dry pyridine as the reaction solvent, which have proved to be much more complicated and less practical than that of Varia et al. (1984) in the present study.

### 3.1.2 Characterization

Thermal analysis of the synthetic product, PMDPH, produced a sharp endothermic peak with a melting point of 172- 174 °C which agrees well with literature reports (Yamaoka et al., 1983). The identity of PMDPH was also determined by solution nuclear magnetic resonance spectroscopy (Fig. 11). 1.0 (t, CH<sub>3</sub>), 2.3 (q, CH<sub>2</sub>), 5.5 (s, CH<sub>2</sub>), 7.4 (m) and 9.9 ppm (s, NH).

## 3.2 Characterization of DPH crystals grown from methanol

### 3.2.1 Crystal morphology, particle size and crystallization yield

Crystallization of DPH from methanol in the absence of PMDPH produced crystals in the form of acicular prisms. The presence of PMDPH in the crystallization media at concentrations exceeding 3 g L<sup>-1</sup> afforded long, thin platy crystals, as determined by SEM (Figs. 12-16). The extent of the habit changes depended on the concentration of PMDPH present. The changes in crystal habit were accompanied by a slight decrease in the mean particle size and an increase in the specific surface area of the DPH crystals (Fig. 17). However, two-dimensional image analysis of the DPH crystals indicated that the length-to-width ratios of the crystals did not change significantly with changes in crystal habit and particle size. This suggests that the additive preferentially inhibits growth of the DPH crystals along the third dimension, probably by

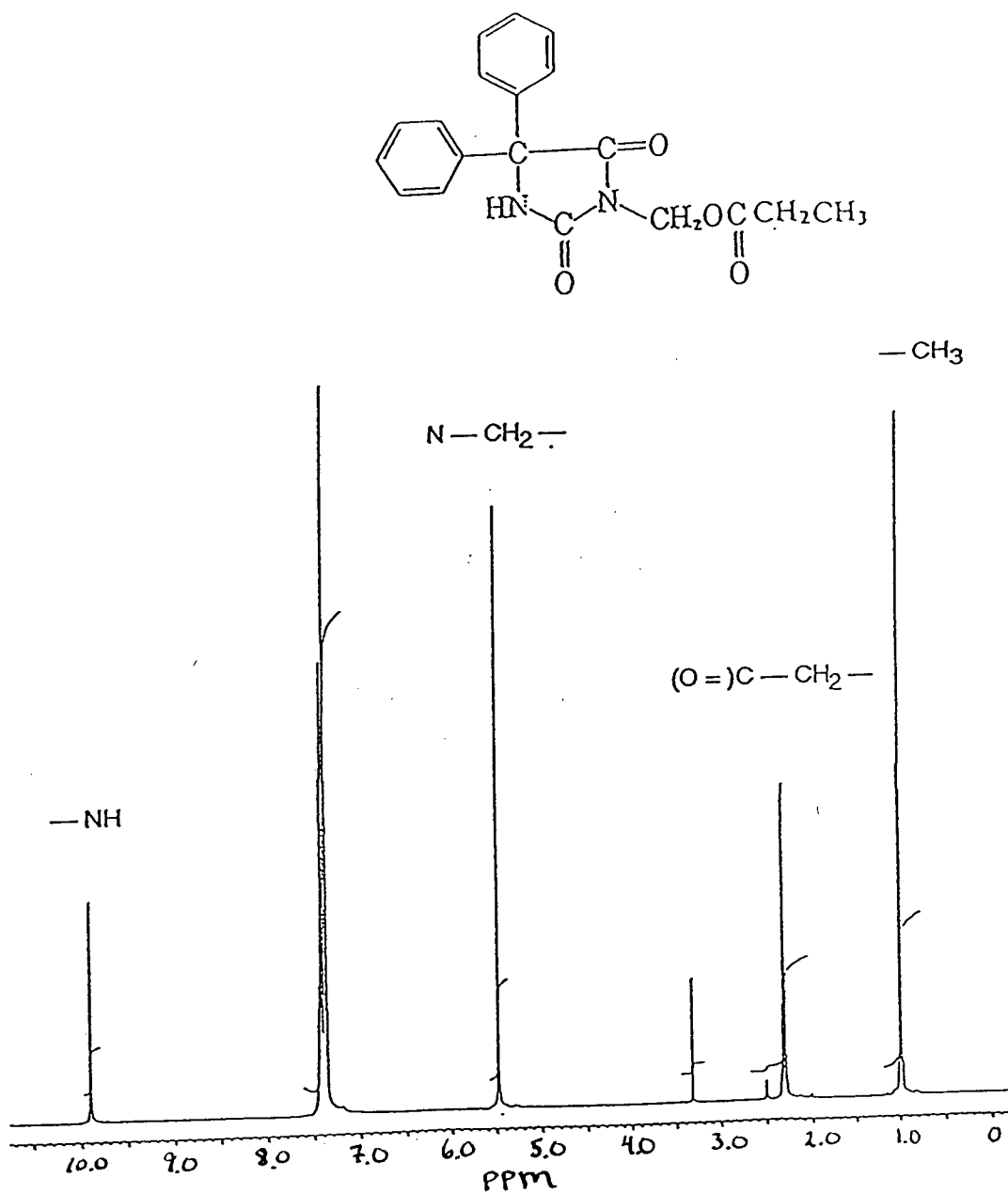


Fig. 11 400 MHz  $^1\text{H}$ -NMR spectrum of PMDPH.

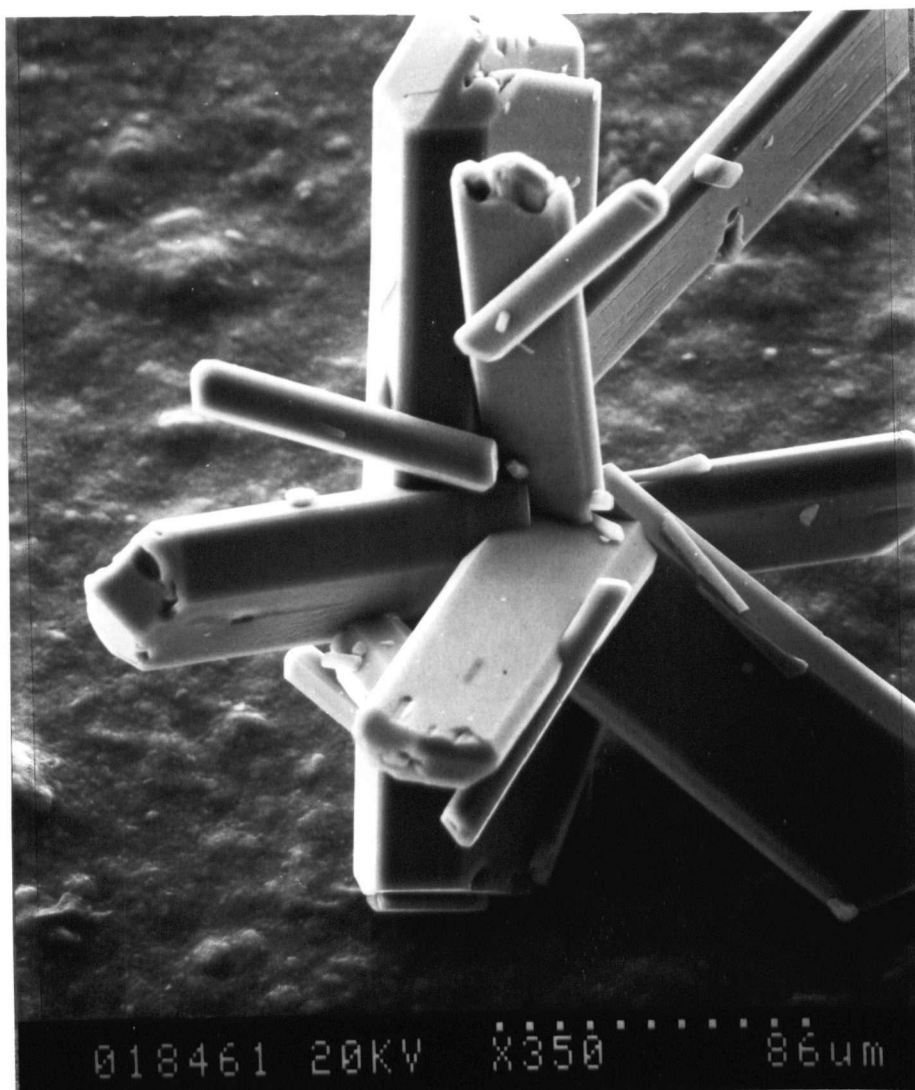


Fig. 12 Scanning electron photomicrograph of DPH crystallized from methanol in the absence of PMDPH.

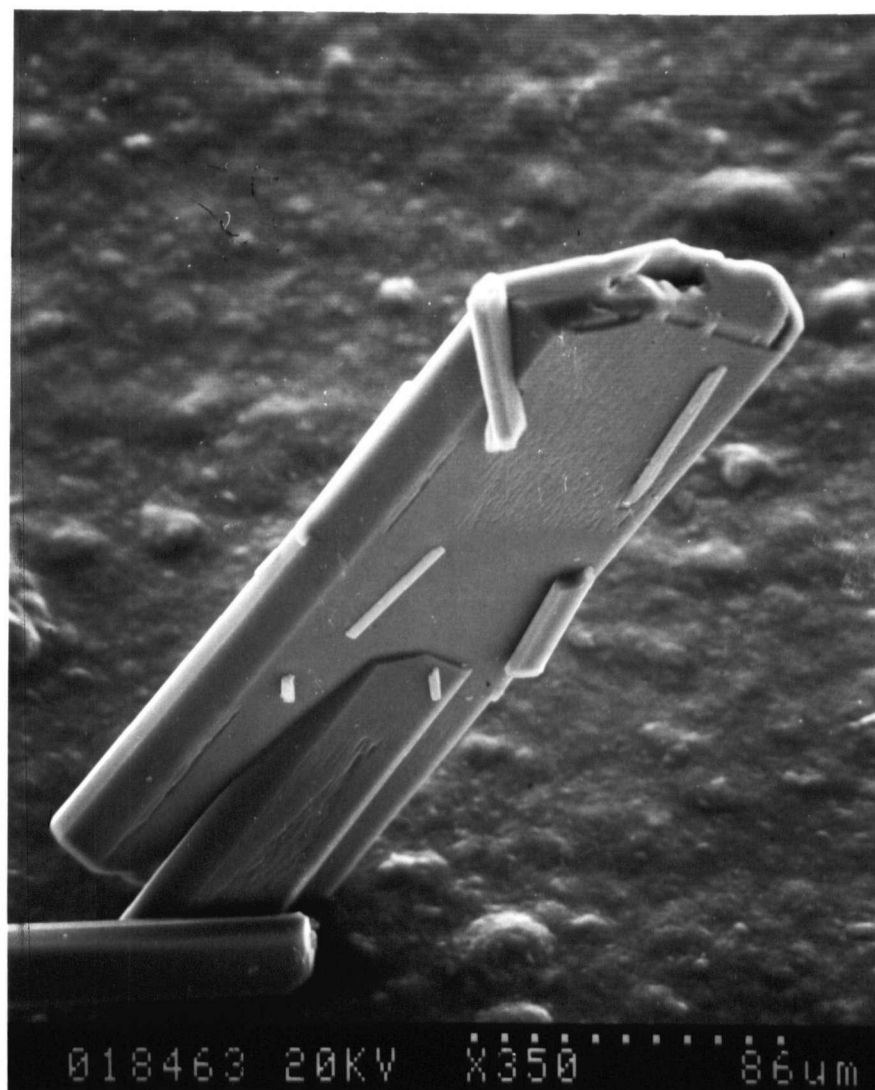


Fig. 13 Scanning electron photomicrograph of DPH crystallized from methanol in the presence of  $1 \text{ g L}^{-1}$  PMDPH.



Fig. 14 Scanning electron photomicrograph of DPH crystallized from methanol in the presence of 3 g L<sup>-1</sup> PMDPH.



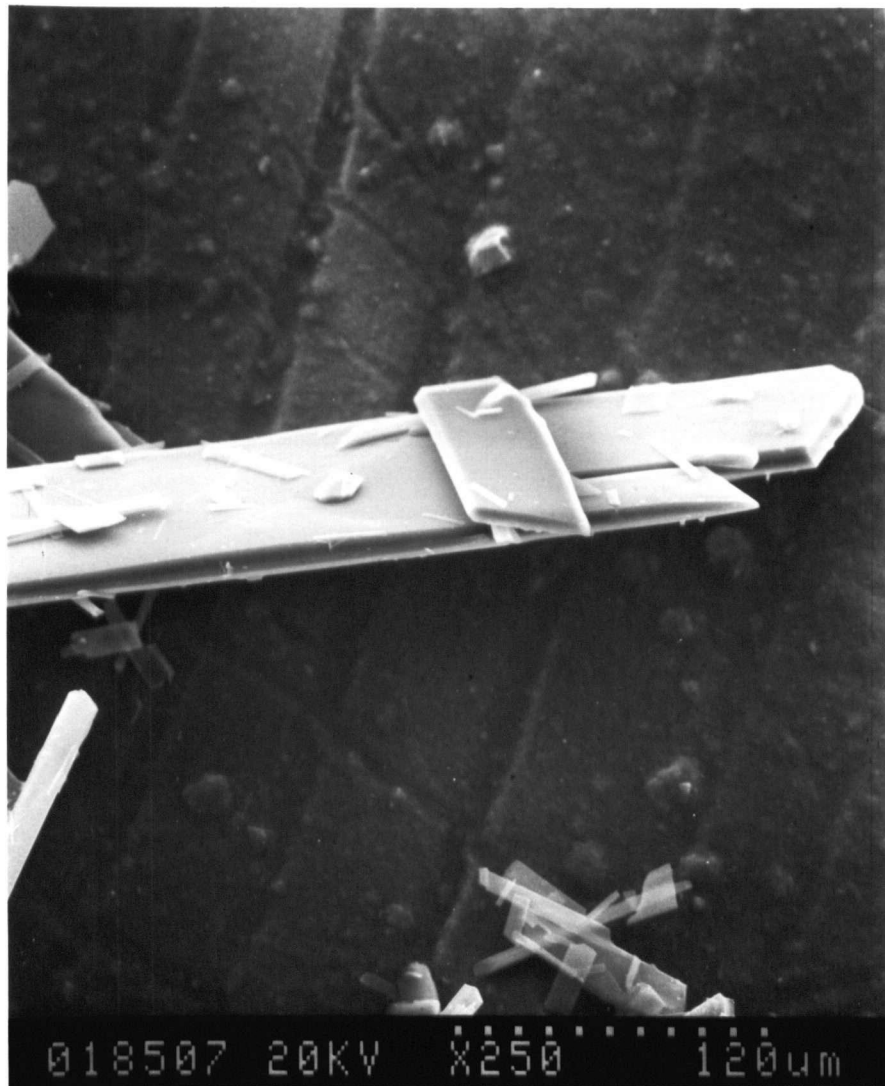


Fig. 15 Scanning electron photomicrograph of DPH crystallized from methanol in the presence of 5 g L<sup>-1</sup> PMDPH.



Fig. 16 Scanning electron photomicrograph of DPH crystallized from methanol in the presence of 7 g L<sup>-1</sup> PMDPH.

adsorbing on to the corresponding crystallographic faces where its interactions with the DPH are likely to be more energetically favorable and thus to be stronger. The strength of such interactions may be related to the polarity of the faces, the extent of hydrogen bonding or the packing arrangement of the DPH molecules along these surfaces (i.e., steric factor). These results are consistent with those known for the effects of additive adsorption on the relative growth rate of crystal faces (see Section 1.2.2). Davey (1979) suggested that the adsorbed additive could impede the growth process by a variety of mechanisms depending on the site of adsorption (see Fig. 1). Adsorbed additive molecules could either interfere with the movement of the growth step across the crystal face when this process is the rate determining step for crystal growth (i.e., at high supersaturations) or influence the velocity at which the edges of the surface nuclei spread, when the formation of nuclei is rate determining (i.e., at low supersaturations) (Davey, 1979). Davey (1979) further suggested that the additive could be incorporated into the growing crystal, especially if there is some lattice similarity, or interact chemically with the crystal surface to selectively alter the surface free energies of different faces.

The notion that the presence of PMDPH retards the crystal growth of DPH is further substantiated by an attendant reduction in crystallization yield collected at two hours after seeding ( $F(7,16)=24.931$ ,  $p<0.05$ ) (Fig. 18). Since the solubility of DPH in methanol at 30 °C was not altered by the presence of PMDPH (up to 7 g L<sup>-1</sup>), the observed change in crystallization yield could not be attributed to a change in the initial degree of supersaturation of the crystallization solutions. Such a change would have affected the overall driving force in the crystallization process (see Eqn. 5, Section 1.2.1.2).

Chow and Hsia (1991) observed similar results with DPH crystals grown in the presence of AMDPH. AMDPH also preferentially inhibited the growth of

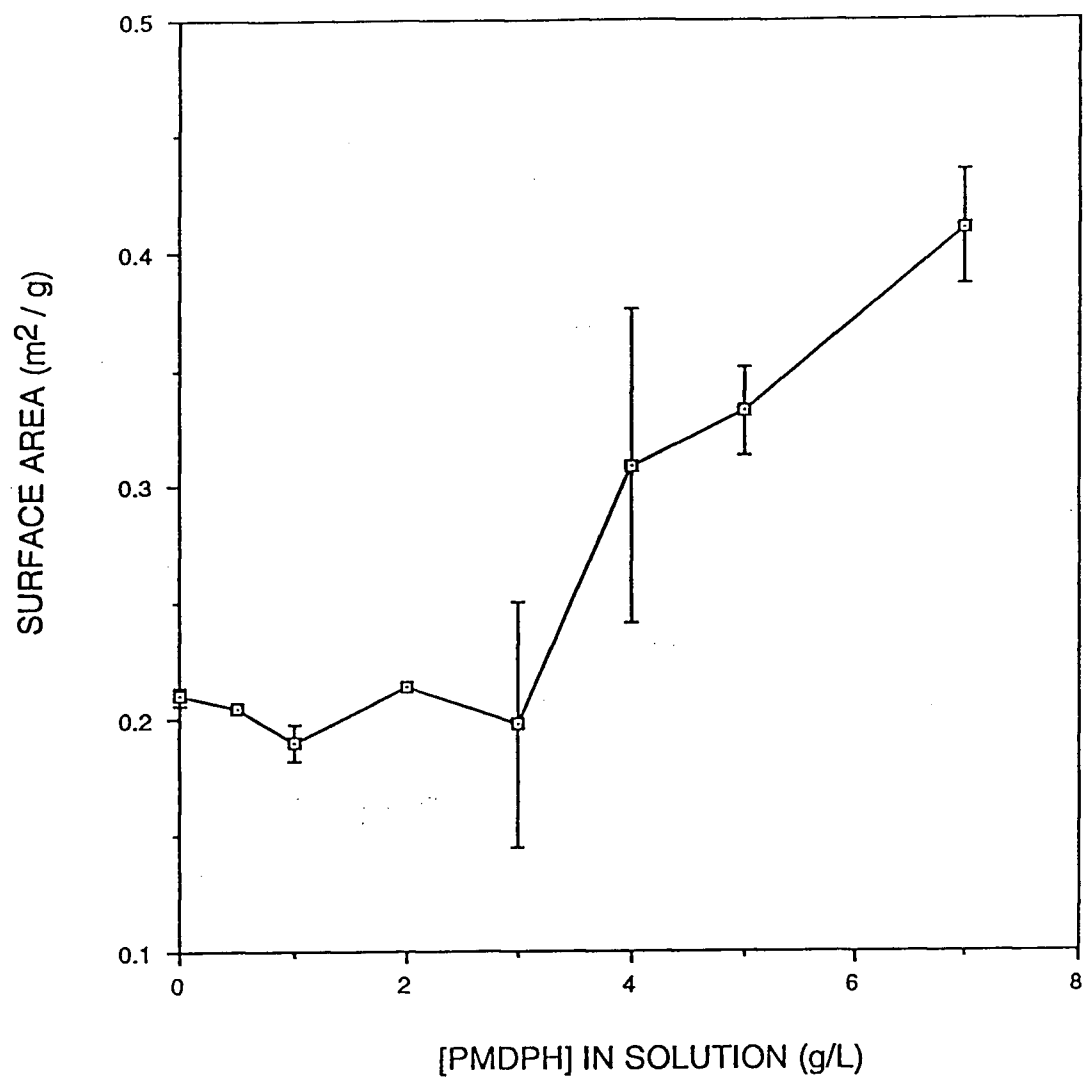


Fig. 17 Specific surface areas of DPH crystallized from methanol containing various concentrations of PMDPH. The vertical bars represent the standard deviations of 2 separate batches.

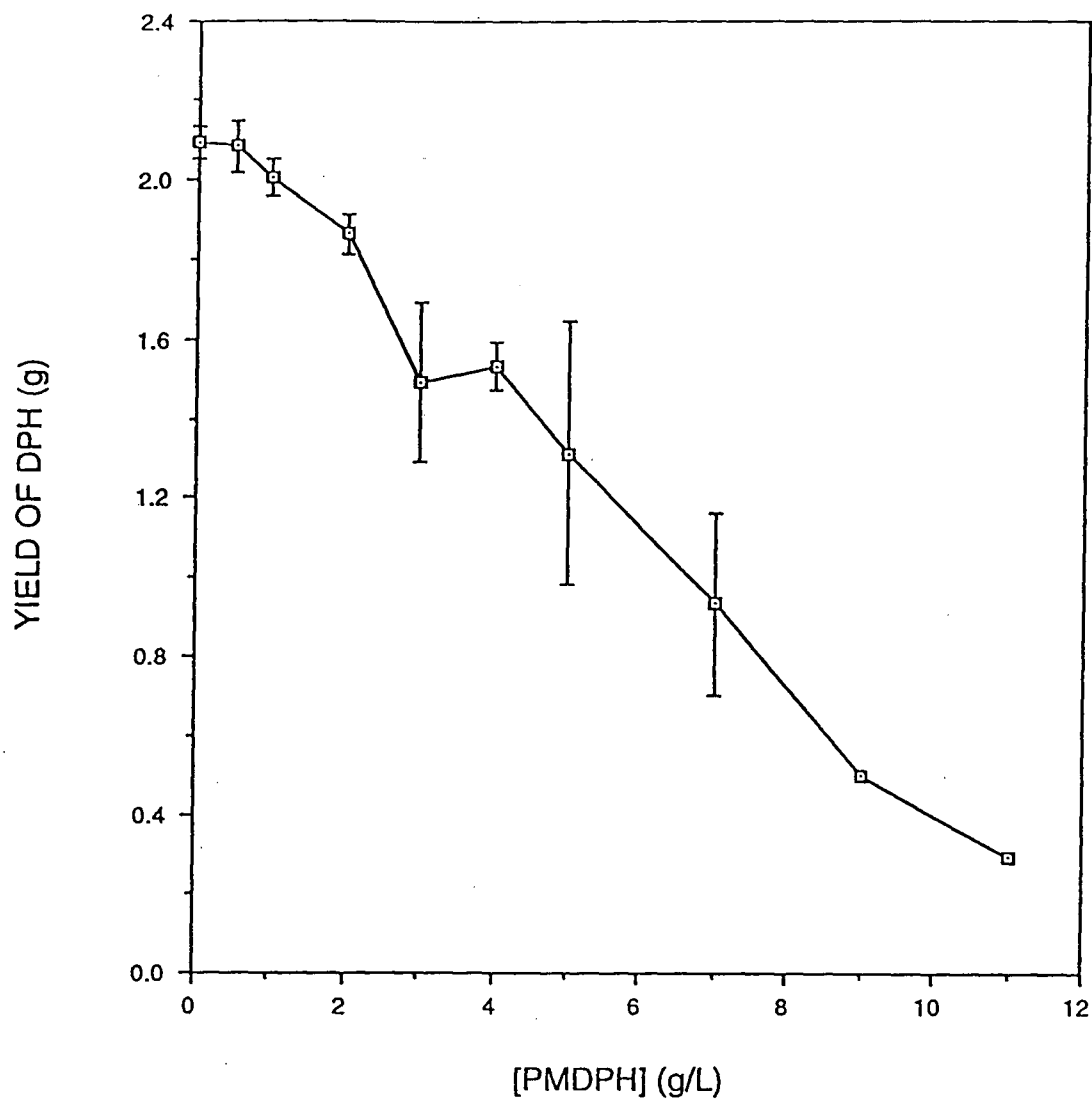


Fig. 18 Yields of DPH crystallized from methanol containing various concentrations of PMDPH. The vertical bars represent the standard deviations of 4 separate batches.

certain faces of the DPH crystals. However, concentrations of at least  $5 \text{ g L}^{-1}$  were necessary to produce a noticeable change in either the crystal habit or crystallization yield. This suggests that AMDPH is a less potent habit modifier than PMDPH, possibly due to weaker interactions with the crystal faces and/or stronger interactions with the solvent. To verify this latter point, the solubilities of three ester homologues of DPH, namely, AMDPH, PMDPH and 3-butanoyloxymethyl-5,5-diphenylhydantoin (BMDPH) were determined in methanol at  $30^\circ\text{C}$ . The solubilities of these compounds in methanol were found to correlate well with their melting points. In line with this correlation, AMDPH has a higher solubility in methanol (the crystallization solvent) than PMDPH (Fig. 19) (Chow, 1991), suggesting that AMDPH interacts more strongly with methanol than PMDPH.

Another notable difference in the effects between AMDPH and PMDPH is the apparent difference in the appearance of the additive-treated crystal surfaces. The crystals grown in the presence of high concentrations of AMDPH ( $9\text{--}12 \text{ g L}^{-1}$ ) appear to have 'rugose' surfaces which were not observed for the crystals grown in the presence of PMDPH. This suggests that AMDPH may be more disruptive than PMDPH in terms of inducing 'rugosity' or structural defects on the crystal surface of DPH.

### 3.2.2 Retention of methanol by DPH crystals

The solvent used in solution-phase crystallization may be considered to be a huge source of impurities (Davey, 1979). With this in mind, the amount of methanol present in the DPH samples was measured by gas chromatography. Analysis of various crystal samples revealed that they contained negligible amounts of methanol (7 - 16 ppm) with respect to the amount of PMDPH present

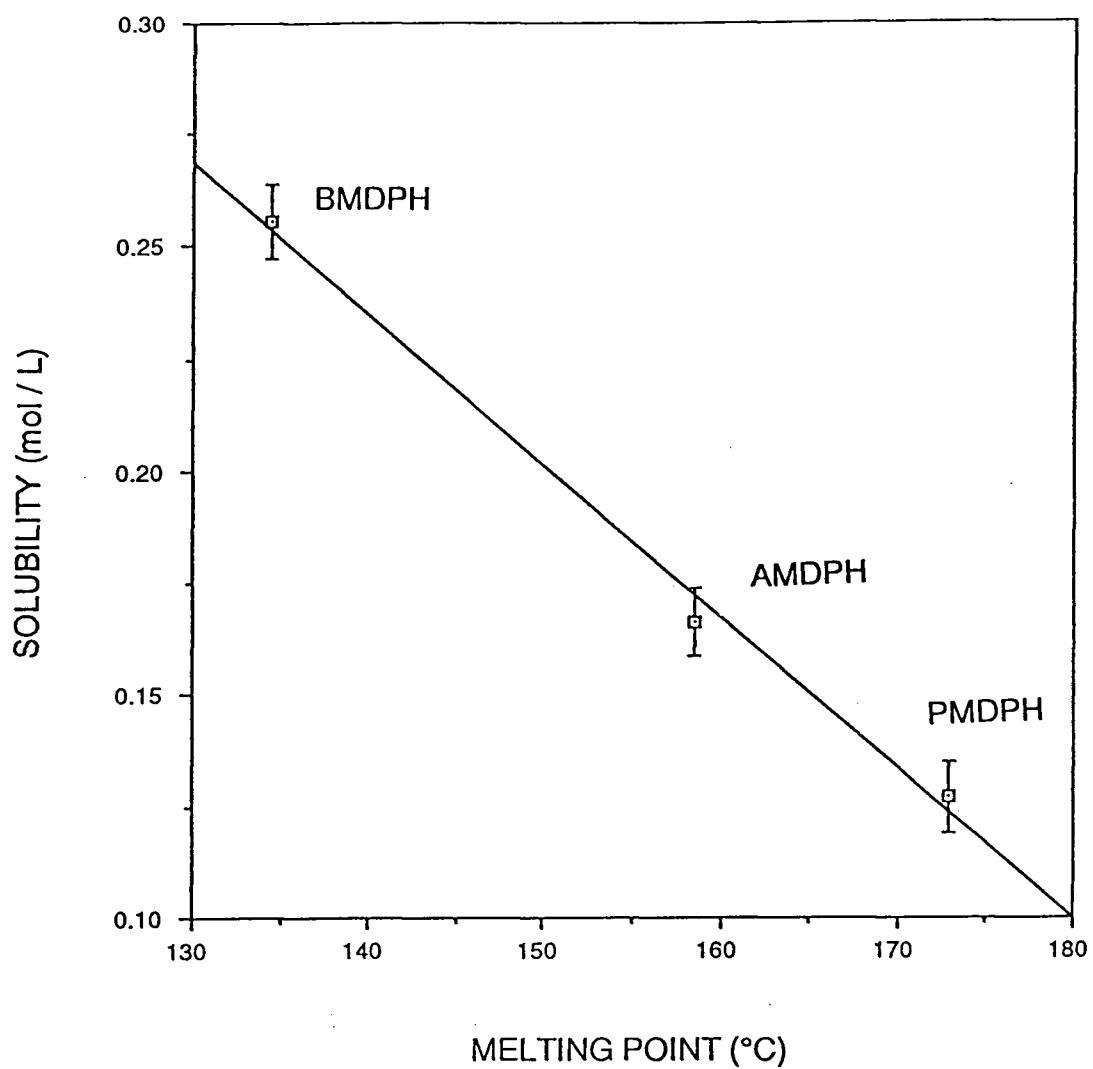


Fig. 19 Linear regression plot of the solubility of three methyl esters of DPH in methanol at 30 °C against their respective melting points. The vertical bars represent the standard deviations of 8 determinations.

and thus, the effects of methanol could be considered to be negligible in the present study.

### 3.2.3 Sorption of PMDPH by DPH crystals

The sorption of PMDPH by DPH crystals was found to increase linearly with increasing concentrations of PMDPH in the crystallization media over the range of 0.5 - 11 g L<sup>-1</sup> of PMDPH (Fig. 20). In order to determine the amount of PMDPH adsorbed on the surface of the crystals, doped crystals prepared at 3, 5, 7 g L<sup>-1</sup> PMDPH were subjected to repeated vigorous washings (four separate washes) with 5 % methanol in water. This washing treatment removed 69±2, 72±2 and 50±2 % w/w of PMDPH respectively from these samples while dislodging only 1.0±0.1 % w/w DPH. This indicates that the sorbed additive was predominantly located at or near the surface of the crystals. Interestingly, the amount of PMDPH sorption increased linearly with increasing concentration of PMDPH in the solutions over both the ranges, 0 - 3 g L<sup>-1</sup>, where the specific surface area of the samples remained unchanged, and 3 - 7 g L<sup>-1</sup>, where significant increases in surface area were observed (Fig. 17). Similar studies on the AMDPH-doped crystals prepared at comparable additive concentrations (Chow and Hsia, 1991) indicated that 51±8 % w/w of the sorbed AMDPH resided at or near the surface of the DPH crystals. The difference in surface adsorption observed between the two additives appears to be unrelated to differences in the surface area of the respective doped crystals since the latter differences are insignificantly small. These observations together with the observed differences in solubility between AMDPH and PMDPH suggest that the addition of a methylene group to the ester side chain of the DPH ester homologues reduces their interaction with the crystallization solvent and thereby enhances their interaction with the crystal surface of DPH.



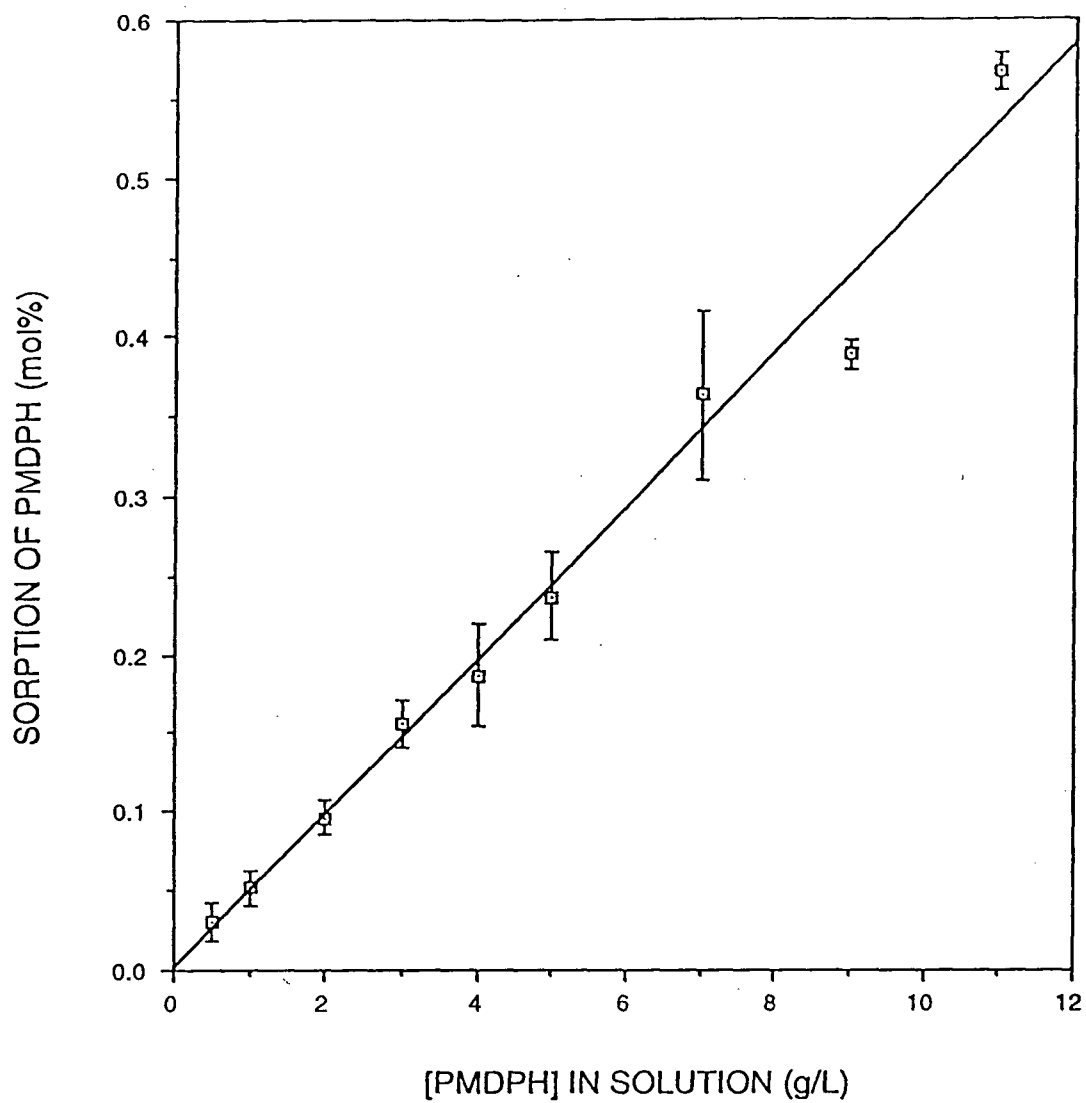


Fig. 20 Sorption of PMDPH by DPH crystals grown from methanol containing various concentrations of PMDPH. The vertical bars depict the standard deviations of quadruplicate determinations.

The two aforementioned DPH-additive systems differ from the earlier work of a similar nature undertaken with acetaminophen (Chow et al., 1985) in that very little of the sorbed additive (*p*-acetoxyacetanilide) in the acetaminophen study is present at or near the surface of the crystals. This difference may be attributed to the necessity of employing much higher concentrations (~ six times more) of the additive, AMDPH or PMDPH, in the crystallization media to promote modification of the habit and physical properties of the DPH crystals. This requirement may be explained by the relatively strong DPH-DPH interactions, or by the stronger interactions between the additive and the solvent. As mentioned in Section 1.3.3.1, solid solubility is unlikely to occur if the additive incorporation disrupts the hydrogen bonding network of the host crystal (Kitaigorodsky, 1984). As a result of the unfavorable energy change associated with such substitution, the additives may have a greater tendency to interact with DPH at the surface of the crystals as opposed to being incorporated into the crystal lattice. In terms of the differences in solubility and surface adsorption between the two ester homologues of DPH, one would expect a greater propensity for AMDPH than for PMDPH to remain in solution, and therefore, less AMDPH to adsorb onto the crystal surfaces.

While the sorption of AMDPH by the DPH crystals appears to be similar in trend to that of *p*-acetoxyacetanilide by the acetaminophen crystals in that both exhibit a plateau above a certain concentration of additive in the solutions (Chow and Hsia, 1991), the sorption of PMDPH by the DPH crystals displayed a linear increase with in the concentration range of PMDPH employed in the crystallization media (0 - 11 g L<sup>-1</sup>) (Fig. 20).

### 3.2.4 Powder X-ray diffraction analysis

The powder X-ray diffraction patterns of the various DPH samples revealed no significant differences in either the diffraction pattern or d-spacing values ( $<0.5\%$ ), indicating that PMDPH did not promote gross crystalline modification such as polymorphism (Fig. 21). This point is further substantiated by the absence of any change in the equilibrium solubility between the various DPH samples in water at  $30\text{ }^{\circ}\text{C}$  ( $F(2,9)=3.513$ ,  $p>0.05$ ) (Table 1). The absence of major structural changes and the similarities in size and structure between the additive and DPH suggest that the trace additive may be present in the DPH crystals in the form of a substitutional solid solution. As discussed in Section 1.3.3, two types of substitutional solid solutions are possible for organic crystals, namely, true and interblock substitutional solid solutions. For the formation of a true substitutional solid solution, the additive must at least be able to partially maintain the hydrogen bonding network of DPH. This would seem feasible for PMDPH because it retains all of the hydrogen bond acceptor sites and one of the two donor sites of DPH, thus allowing limited solubility and limited changes in the crystal lattice of DPH which may be too small to be detected by powder X-ray diffraction. The formation of an interblock solid solution requires only that there be partial geometrical conformity between the impurity and host molecules. In such a solid solution the additive molecules either occupy defect sites within the crystals or are located at the boundaries of mosaic blocks. Since these occupation sites are rarely the lattice positions, the presence of the additive is unlikely to alter the unit cell parameters of the host crystal. In any case, as alluded to in Section 1.3.3.2, a small amount of impurity uptake into a crystal can result in an overall decrease in the energy of the system and hence a more stable crystal.

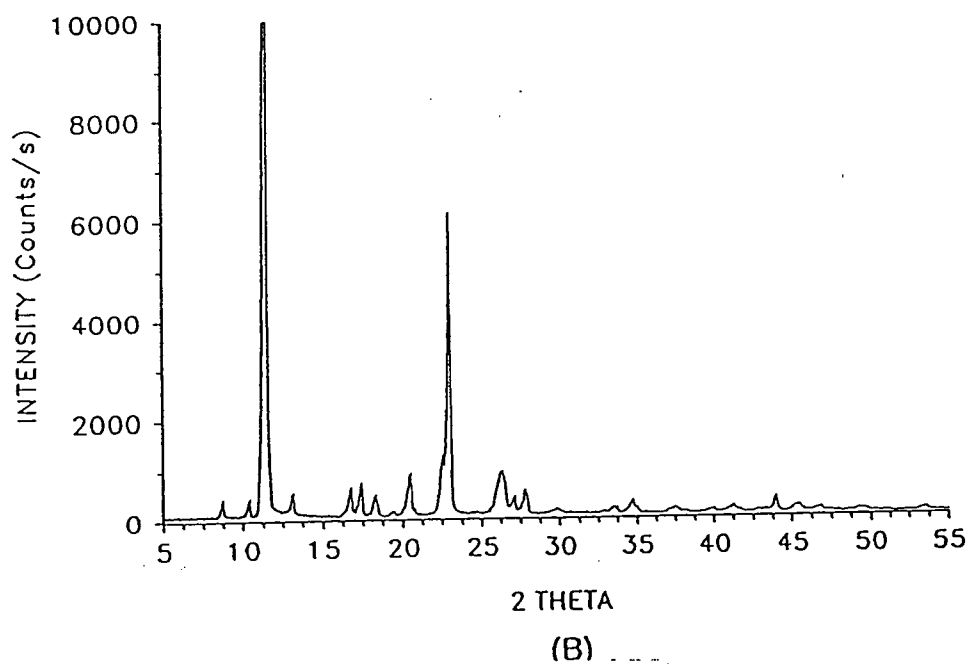
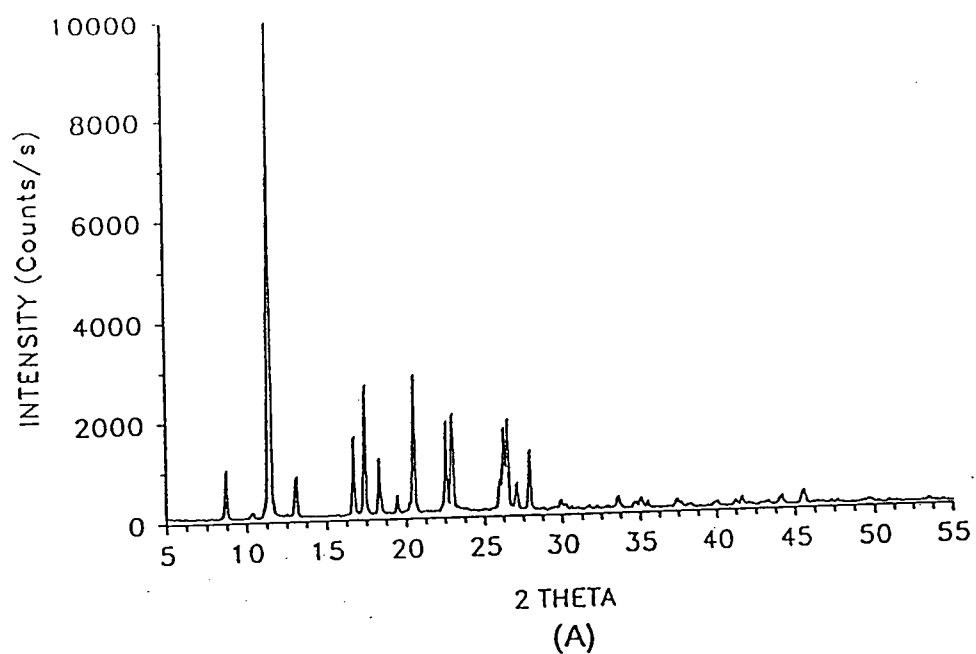


Fig. 21 Powder X-ray diffraction pattern of DPH crystals grown from methanol containing (A) 0 g L<sup>-1</sup> PMDPH; and (B) 11 g L<sup>-1</sup> PMDPH.

DPH crystals grown from methanol in the presence of the following concentrations of PMDPH (g L <sup>-1</sup> ):	Equilibrium solubility (µg/mL)
0	31.7 ± 1.0
4	29.7 ± 2.3
7	32.4 ± 0.4

Table 1      Equilibrium solubility of DPH crystals grown from methanol containing various concentrations of PMDPH in water at 30 °C.

### 3.2.5 Thermal analysis

Differential scanning calorimetric studies revealed that the sorption of PMDPH by the DPH crystals slightly reduced their melting point ( $F(9,44)=1.357$ ,  $p>0.05$ ),  $T_m$ , but significantly decreased their enthalpy of fusion ( $F(9,42)=4.927$ ,  $p<0.05$ ),  $\Delta H^f$ , and entropy of fusion ( $F(9,42)=4.805$ ,  $p<0.05$ ),  $\Delta S^f$ , by as much as 8 % for the samples prepared at  $11 \text{ g L}^{-1}$  PMDPH (Figs. 22, 23; Table 2). This suggests that the presence of PMDPH augments both the enthalpy and entropy of the crystals (see Section 3.6.1 below).

#### 3.2.5.1 Thermodynamic interpretation

The thermodynamic properties depicting the fusion process at constant atmospheric pressure,  $p$ , may be expressed as follows:

$$\Delta H^f = \Delta U^f + p\Delta V^f \quad (10)$$

$$\Delta G^f = \Delta H^f - T_m \Delta S^f \quad (11)$$

where the enthalpy of fusion,  $\Delta H^f = H_{\text{liquid}} - H_{\text{solid}}$ ; the internal energy change,  $\Delta U^f = U_{\text{liquid}} - U_{\text{solid}}$ ; the change in molar volume upon fusion,  $\Delta V^f = V_{\text{liquid}} - V_{\text{solid}}$ ; the entropy of fusion,  $\Delta S^f = S_{\text{liquid}} - S_{\text{solid}}$ ; and  $T_m$  is the melting temperature. Fusion is a reversible process at  $T_m$  therefore the free energy of fusion,  $\Delta G^f$ , is zero and

$$\Delta S^f = \Delta H^f / T_m \quad (12)$$

Since the observed changes in  $T_m$  for the DPH samples are very small compared to those observed in  $\Delta H^f$ , Equation 12 indicates that the changes in

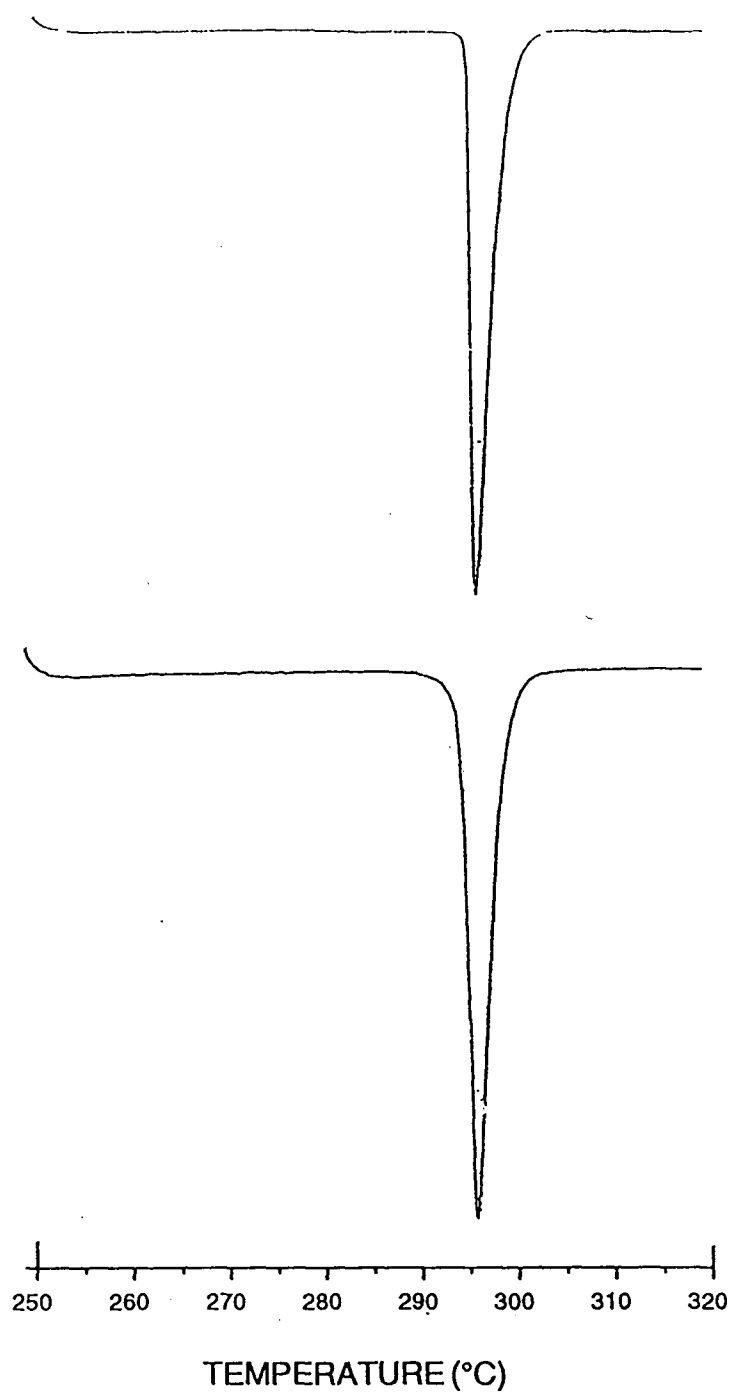


Fig. 22 Differential scanning calorimetric thermograms of DPH crystals grown from methanol containing (A) 0 g L<sup>-1</sup> PMDPH; and (B) 7 g L<sup>-1</sup> PMDPH.

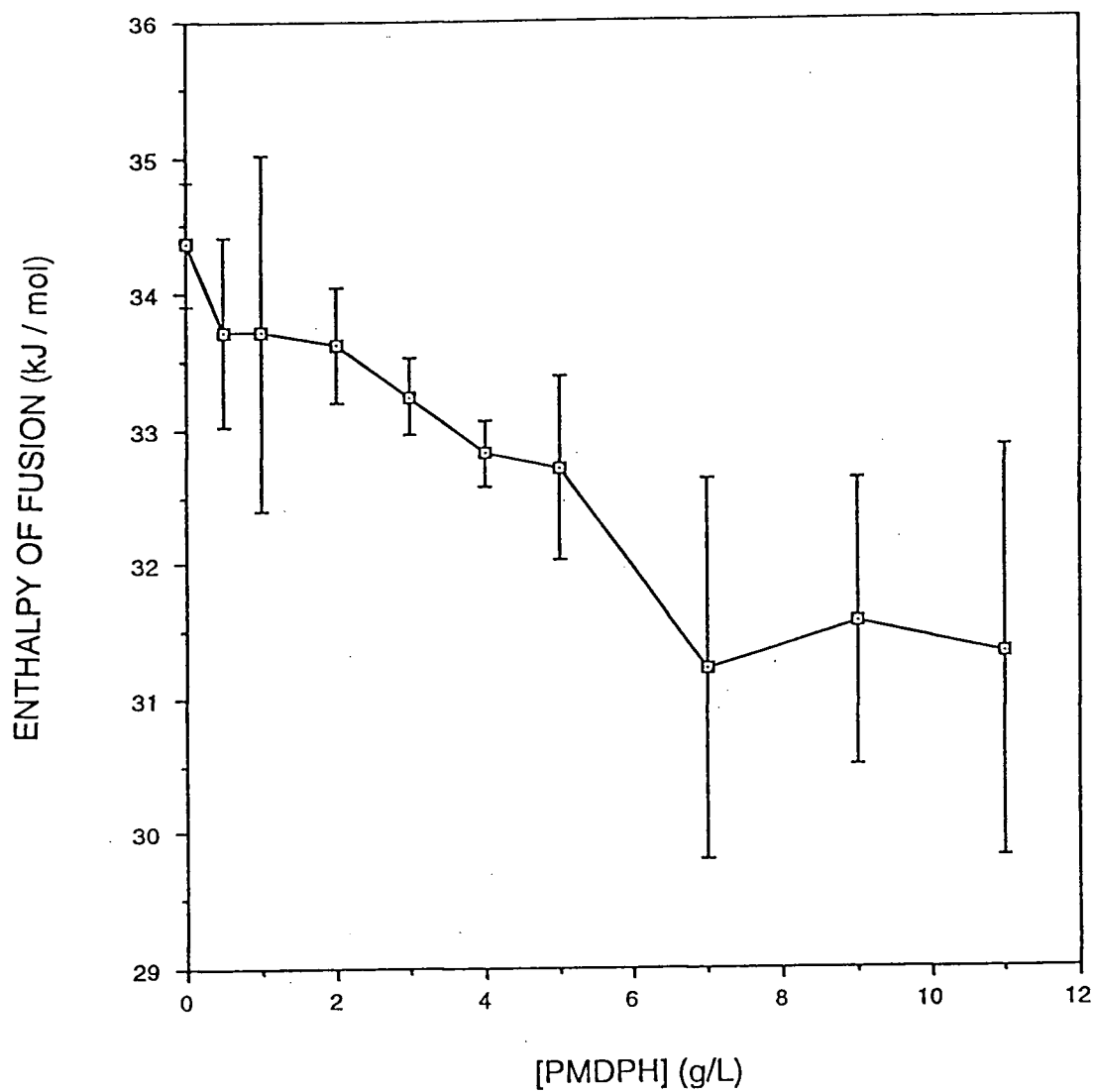


Fig. 23 Enthalpies of fusion,  $\Delta H_f$ , of DPH crystals grown from methanol in the presence of various concentrations of PMDPH. The vertical bars represent the standard deviations of 6-10 determinations.



[PMDPH] (g L <sup>-1</sup> )	x <sub>P</sub> x 10 <sup>4</sup>	T <sub>m</sub> ± s.d. (K)	ΔH <sup>f</sup> ± s.d. (kJ mol <sup>-1</sup> )	ΔS <sup>f</sup> ± s.d. (J K <sup>-1</sup> mol <sup>-1</sup> )	S <sub>P</sub>	S <sub>D</sub>	ΔS <sub>ideal</sub>
0	0	568.6 ± 0.1	34.4 ± 0.4	59.9 ± 0.1	0	0	0
0.5	3.0	568.4 ± 0.5	33.7 ± 0.7	59.2 ± 1.2	0.0202	0.0025	0.0227
1.0	5.2	568.4 ± 0.2	33.7 ± 1.3	59.2 ± 2.1	0.0324	0.0043	0.0367
2.0	9.6	568.4 ± 0.2	33.6 ± 0.4	59.3 ± 1.0	0.0554	0.0080	0.0634
3.0	15.6	568.5 ± 0.5	33.2 ± 0.3	58.7 ± 0.1	0.0838	0.0130	0.0968
4.0	18.7	567.9 ± 0.3	32.8 ± 0.2	57.8 ± 0.3	0.0976	0.0155	0.1131
5.0	23.7	568.2 ± 0.3	32.7 ± 0.7	57.7 ± 1.4	0.1190	0.0196	0.1386
7.0	36.2	567.4 ± 0.7	31.2 ± 1.4	55.0 ± 2.5	0.1695	0.0301	0.1996
9.0	38.9	568.0 ± 0.2	31.6 ± 1.1	55.6 ± 1.9	0.1794	0.0323	0.2117
11.0	56.7	567.4 ± 0.2	31.3 ± 1.5	55.2 ± 2.7	0.2437	0.0470	0.2906

Table 2 Mole fraction sorption (x<sub>P</sub>) of PMDPH, melting points (T<sub>m</sub>), molar enthalpies of fusion (ΔH<sup>f</sup>), molar entropies of fusion (ΔS<sup>f</sup> = ΔH<sup>f</sup>/T<sub>m</sub>) of DPH crystals grown from methanol at 0–11 g L<sup>-1</sup> PMDPH, and calculated ideal partial molar entropies (S<sub>j</sub> = -R x<sub>j</sub> ln x<sub>j</sub>), ideal molar entropies of mixing (ΔS<sub>ideal</sub> = ΣS<sub>j</sub>) of the components in the crystals, where P = 3-propanoyloxymethyl-5,5-diphenylhydantoin, D = 5,5-diphenylhydantoin.

$\Delta S^f$  will closely correspond to the changes in  $\Delta H^f$ . Assuming the energetic terms for the liquid state (i.e.,  $H_{\text{liquid}}$ ,  $U_{\text{liquid}}$  and  $S_{\text{liquid}}$ ) are significantly less sensitive to the presence of low concentrations of impurities than those of the highly ordered crystalline state, the decreases observed in  $\Delta H^f$  and  $\Delta S^f$  may be attributed to increases in  $H_{\text{solid}}$  and  $S_{\text{solid}}$  (Chow et al., 1984).

Based on the fundamental assumption that each additive molecule within the DPH crystals modifies the disorder of the crystal lattice and thus exerts the observed effects, a quantitative examination of the changes in entropy may prove to be informative. York and Grant (1985) developed a dimensionless quantity termed 'disruption index' which provides a measure of the disorder induced by a given additive or impurity when present in solid solution in a crystal lattice. The disruption index is given by the slope obtained from the linear regression of the enthalpy of fusion,  $\Delta S^f$ , against the ideal entropy of mixing, as expressed by the following equation:

$$\Delta S^f = \Delta S_o^f - (b - c) \Delta S_{\text{ideal}} \quad (13)$$

where  $\Delta S_o^f$  is the hypothetical entropy of fusion of perfect, uncontaminated crystals,  $b$  and  $c$  are dimensionless proportionality constants which represent the sensitivities of the disordering of the host solid and of the host liquid to simple random mixing with an additive, and  $(b - c)$ , the regression slope, represents the difference between the sensitivity of the entropy of the solid to contamination and that of the liquid, and is known as the 'disruption index' (York and Grant, 1985).  $\Delta S_{\text{ideal}}$  is calculated from the following expression:

$$\Delta S_{\text{ideal}} = -R (x_P \ln x_P + x_D \ln x_D) \quad (14)$$

where  $R$  is the molar gas constant,  $x_P$  is the mole fraction of PMDPH and  $x_D$  is the mole fraction of DPH present in the system.

To evaluate the extent of lattice disruption or disorder induced by PMDPH, the observed  $\Delta S^f$  values were regressed against the ideal molar entropy of mixing values calculated from the crystal compositions. The regression yielded a slope of  $19 \pm 2$  (Fig. 24). According to the previously established basis for this semi-empirical thermodynamic approach (Chow et al., 1985; York and Grant, 1985; Pikal and Grant, 1987; Chow and Hsia, 1991), the value of this slope or of the so-called disruption index indicates that the presence of PMDPH causes about 19 times more disorder and disruption in the crystal lattice of DPH than would be expected from pure random mixing or dilution of the DPH with PMDPH alone, as in an ideal solution. As has been stressed previously (Chow et al., 1985; York and Grant, 1986; Pikal and Grant, 1987; Chow and Hsia, 1991), the  $\Delta S_{\text{ideal}}$  value, which is used as a thermodynamic reference quantity for assessing lattice disorder or disruption, only reflects the entropy change brought about by a random mixing of two closely similar chemical species. Any deviation from this ideal value in a particular situation could indicate a nonrandom or nonuniform distribution of the minor component in the major component, as observed in the present case, or a dissimilarity between the two components in terms of bonding strength and molecular volume. In the present study, since a substantial amount of the additive has been found on the surface of the DPH crystals and since the incorporated additive is likely not uniformly distributed throughout the DPH crystals, the  $\Delta S_{\text{ideal}}$  value probably does not reflect the actual entropy change in the additive sorption process. Nonetheless, the relatively large magnitude of the calculated disruption index indicates that the strong crystal lattice of DPH is sensitive to the presence of traces of PMDPH. The disruptive potential of the

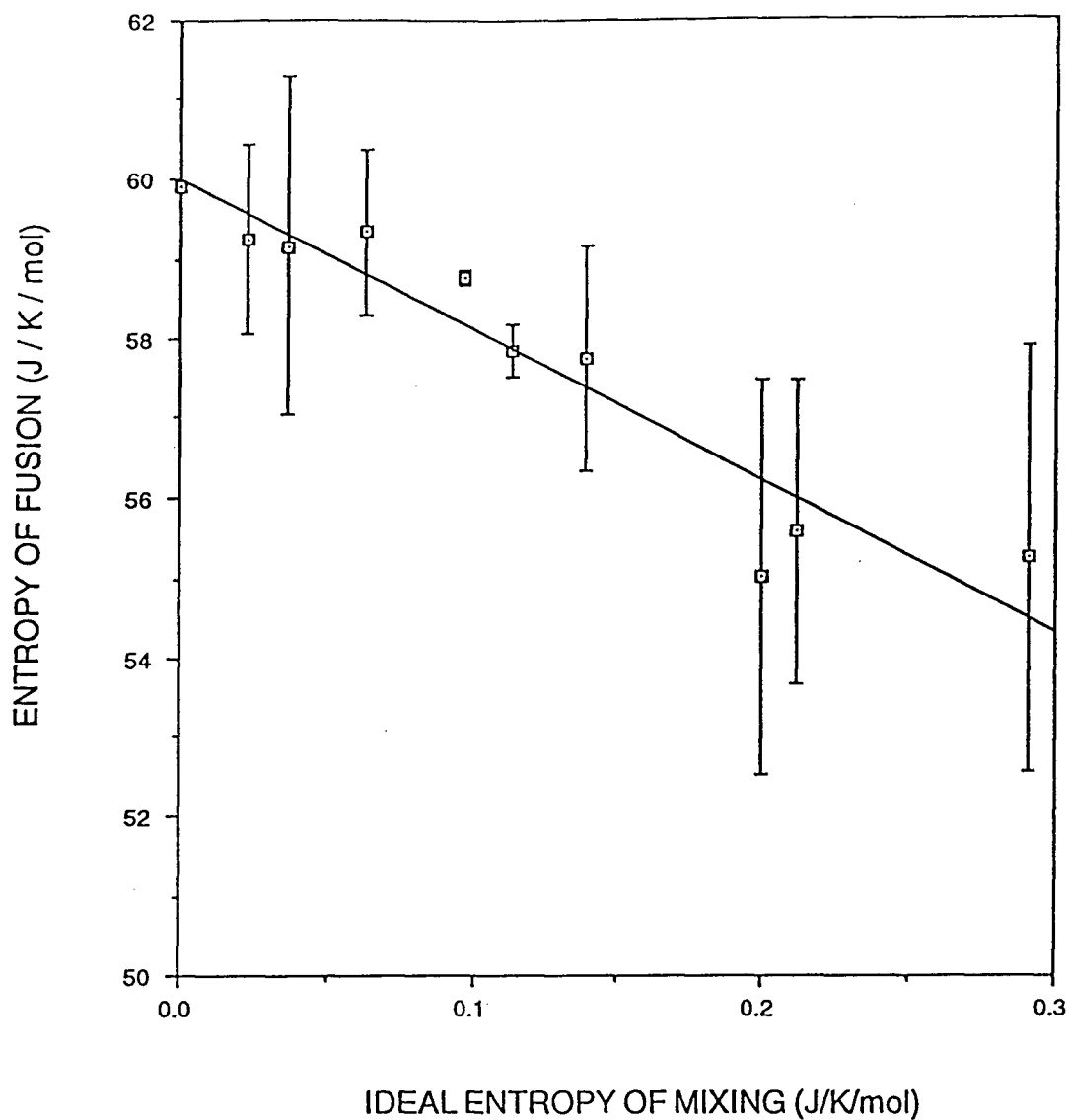


Fig. 24 Linear regression plot of the entropy of fusion,  $\Delta S^f$ , against the ideal molar entropy of mixing,  $\Delta S_{\text{ideal}}$ , for DPH crystals grown from methanol in the presence of various concentrations of PMDPH. The vertical bars depict the standard deviations of 6-10 determinations.

additive is likely due to its ability to disrupt the close molecular packing arrangement and/or the hydrogen bonding pattern within the DPH crystal lattice.

It has been shown in previous studies that the dopant, AMDPH, has a disruption index of  $27 \pm 4$  when retained by the DPH crystals (Chow and Hsia, 1991). A comparison of this value with that obtained for PMDPH ( $19 \pm 2$ ) indicates that AMDPH is capable of generating more intense lattice disruption than PMDPH. However, this latter inference must be viewed with caution in view of the higher proportion of AMDPH being present within the DPH crystals (Chow and Hsia, 1991), as determined by the crystal washing technique described above (Section 2.6). Furthermore, the difference in lattice disruption ability between the two additives, as suggested by the relative magnitude of the disruption indices, is barely significant statistically on account of the fairly large variability in the measured  $\Delta S^f$  values.

### 3.2.6 Dissolution studies

#### 3.2.6.1 Dissolution behavior of PMDPH-doped DPH samples

For the purposes of the present discussion, the data collected within the first 15 minutes of each dissolution run was used to calculate the initial dissolution rate of the crystals, assuming that dissolution occurred essentially under sink conditions during this time period.

The dissolution-time profiles and initial dissolution rates of the DPH crystals grown in the presence of increasing concentrations of PMDPH ( $0.5 - 11 \text{ gL}^{-1}$ ) were determined at both  $25^\circ$  and  $37^\circ\text{C}$  and at a stirring rate of 100 rpm (Figs. 25, 26). The crystal samples displayed progressive and significant increases in both the initial rate ( $F(7,29) = 76.946$ ,  $p < 0.05$ ) and extent of dissolution, up to 3.3 times those of undoped crystals, for samples grown at 7 g

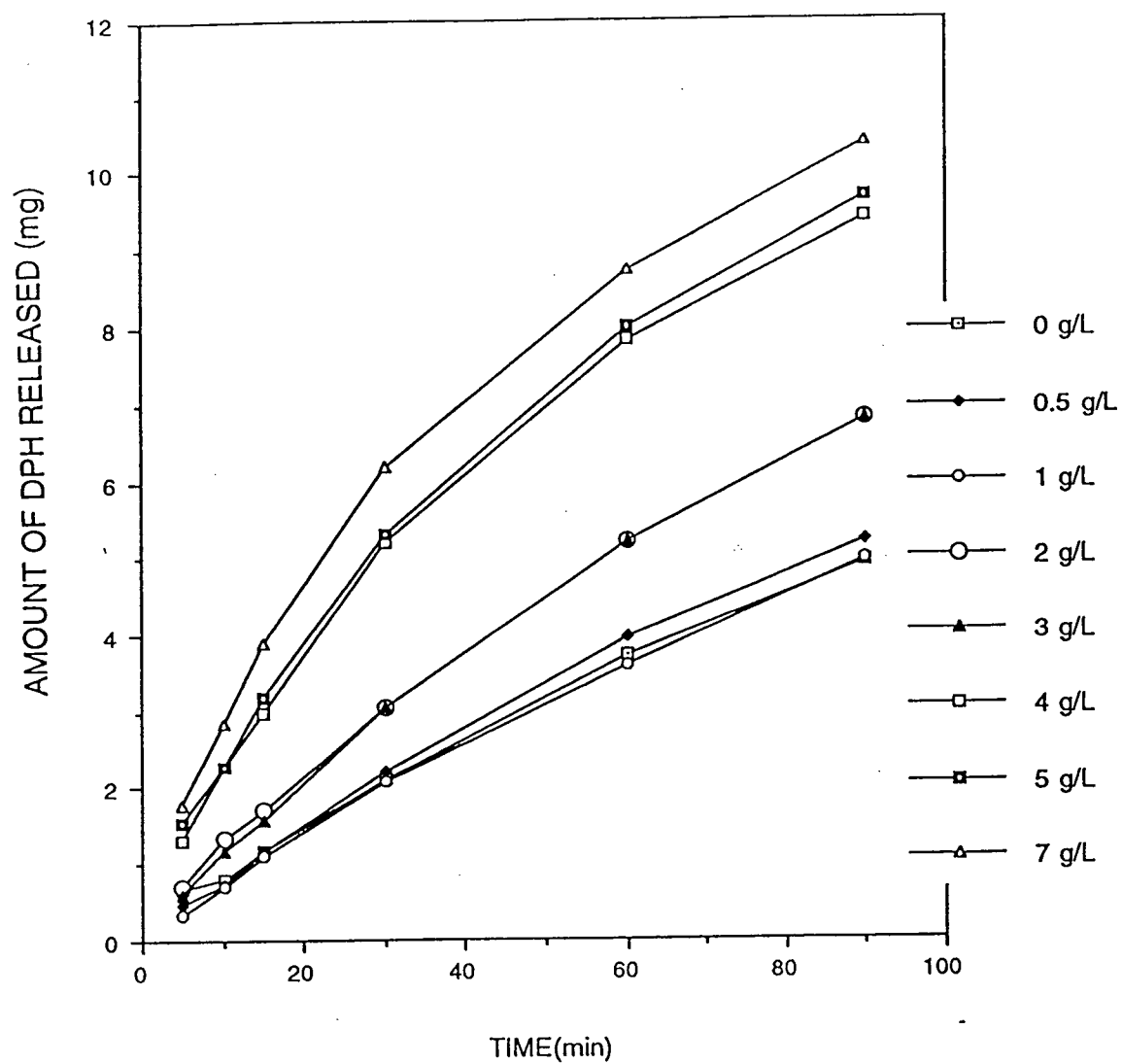


Fig. 25 Dissolution-time profiles at 25 °C of DPH crystals grown from methanol containing various concentrations of PMDPH.

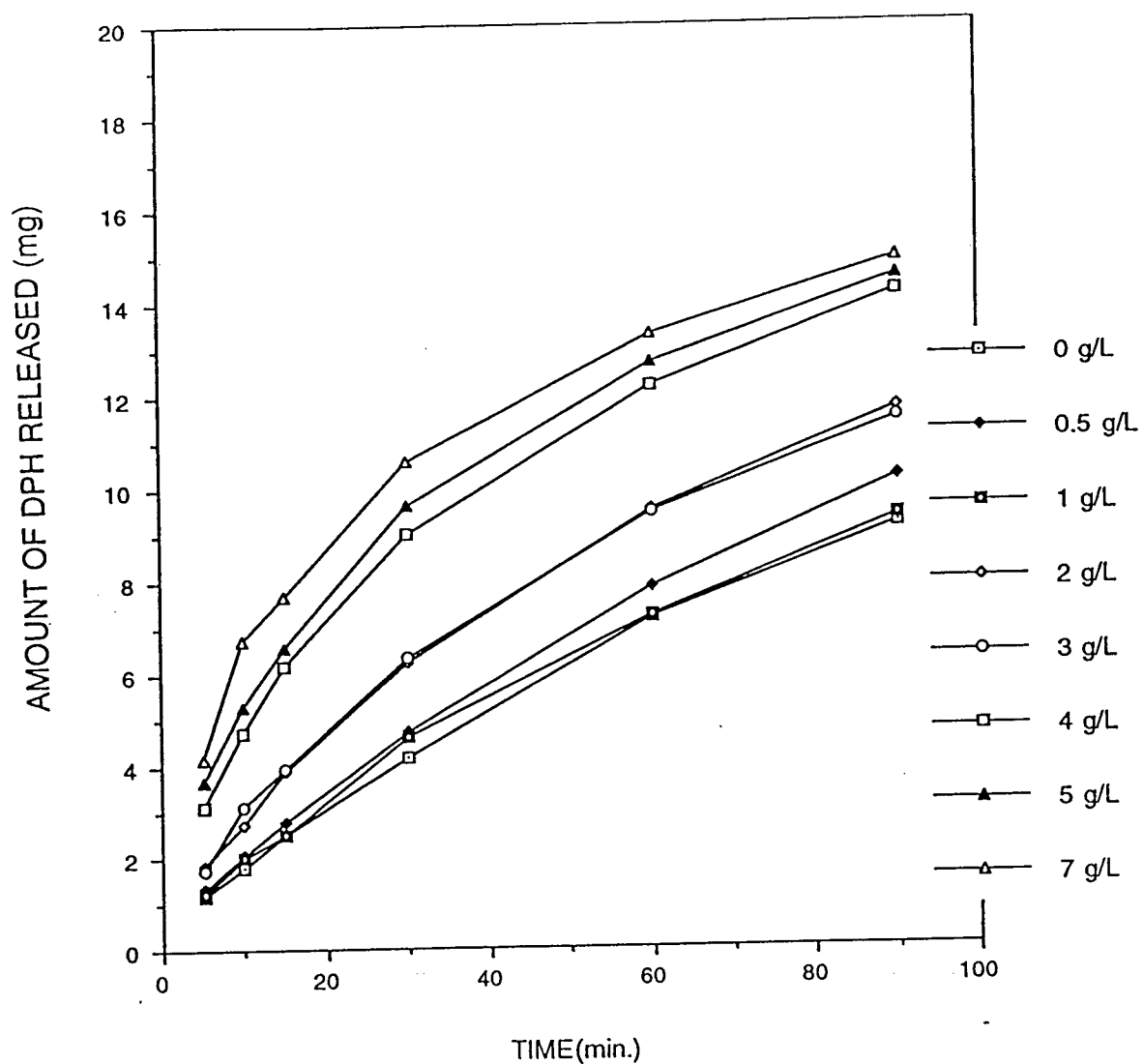


Fig. 26 Dissolution-time profiles at 37 °C of DPH crystals grown from methanol containing various concentrations of PMDPH.

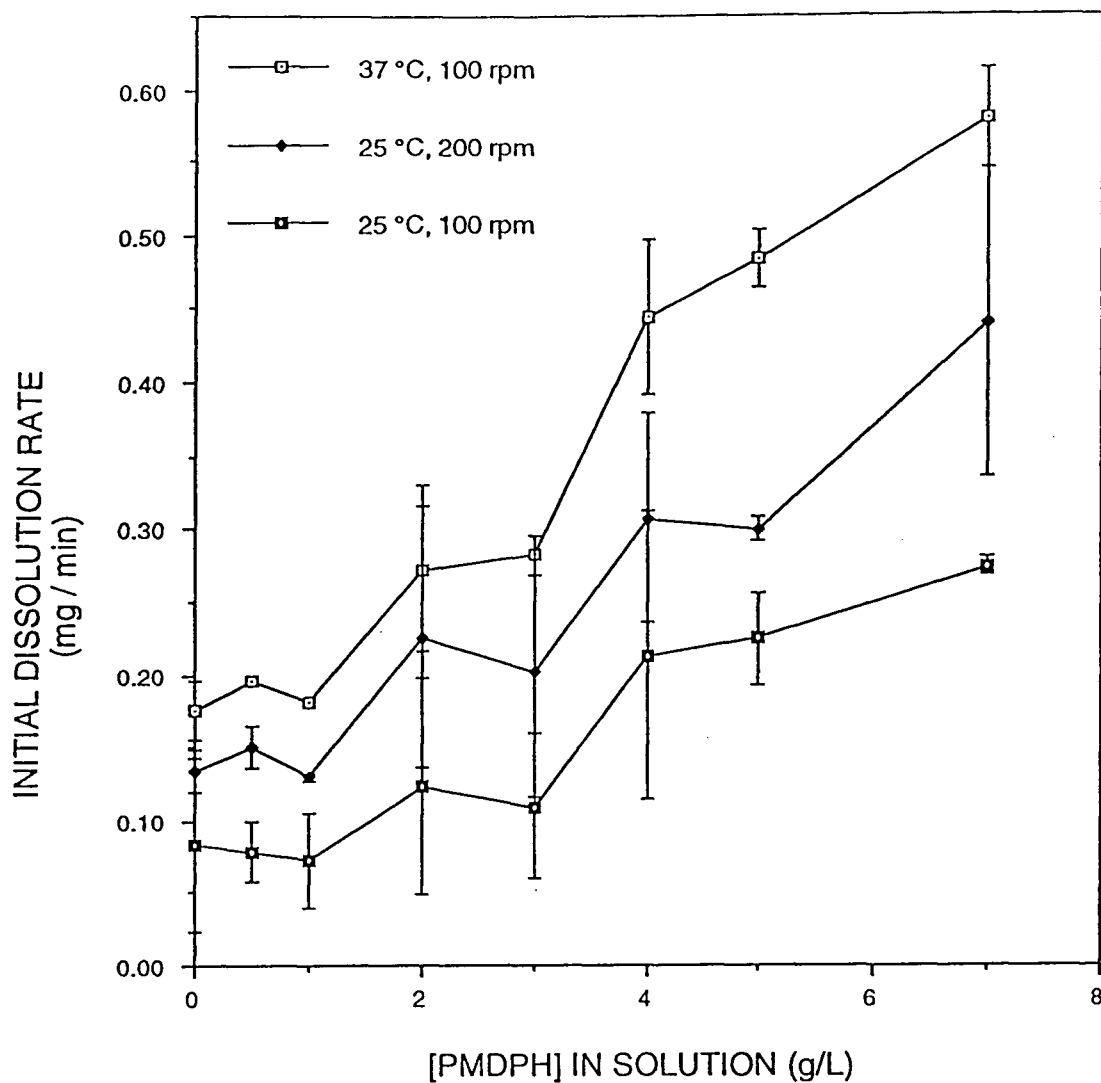


Fig. 27 Initial dissolution rates at 25 ° and 37 °C and at 100 and 200 rpm of DPH crystals grown from methanol containing various concentrations of PMDPH. The vertical bars represent the standard deviations of 6 determinations.



$\text{L}^{-1}$  PMDPH (Fig. 27). To account for the effects of surface area on dissolution, the initial dissolution rate was divided by the initial surface area to give the intrinsic dissolution rate, IDR. With this adjustment for the contribution due to surface area, the IDRs of the crystals at 37 °C still exhibited an increase, reaching a plateau ( $\sim 1.7$  fold increase) for the samples prepared at 3 - 7  $\text{g L}^{-1}$  PMDPH, while the IDRs at 25 °C also displayed a similar but less significant upward trend (Fig. 28). The fact that significant differences in dissolution rate ( $F(7,29) = 17.676$ ,  $p < 0.05$ ) are still observed after adjustment for the differences in surface area indicates that other factors must also be influencing the observed dissolution rates.

The factors most likely involved in the present study are the following: (a) crystal anisotropy; (b) hydrodynamic conditions during dissolution; and (c) crystal defects (see Section 1.3.4.3). Although the effects of crystal anisotropy and habit-related hydrodynamics on the dissolution behavior of crystalline materials are well documented (see Section 1.2.3.2), their contributions appear to be relatively minor in this study since the samples prepared at low concentrations of PMDPH (i.e., 0.5 - 3  $\text{g L}^{-1}$ ) showed very little changes in their specific surface area and habit, while exhibiting significant increases in IDR. Thus, the observed increases in IDR at both 25 ° and 37 °C are likely attributable to defects at the surface and within the bulk of the crystals (Burt and Mitchell, 1981; Chow et al., 1985; Chow and Grant, 1988a; Chow and Grant, 1988b; Chow and Grant, 1989). This has been substantiated by the observed reduction in both the enthalpy and entropy of fusion of the crystals and by the high disruption index ( $19 \pm 2$ ) obtained for the additive. The decreases in  $\Delta H^f$  and  $\Delta S^f$  of the crystals caused by the sorption of PMDPH indicate that the presence of the additive may create both point defects and dislocation defects. The point defects, which merely promote local distortions of the crystal lattice,

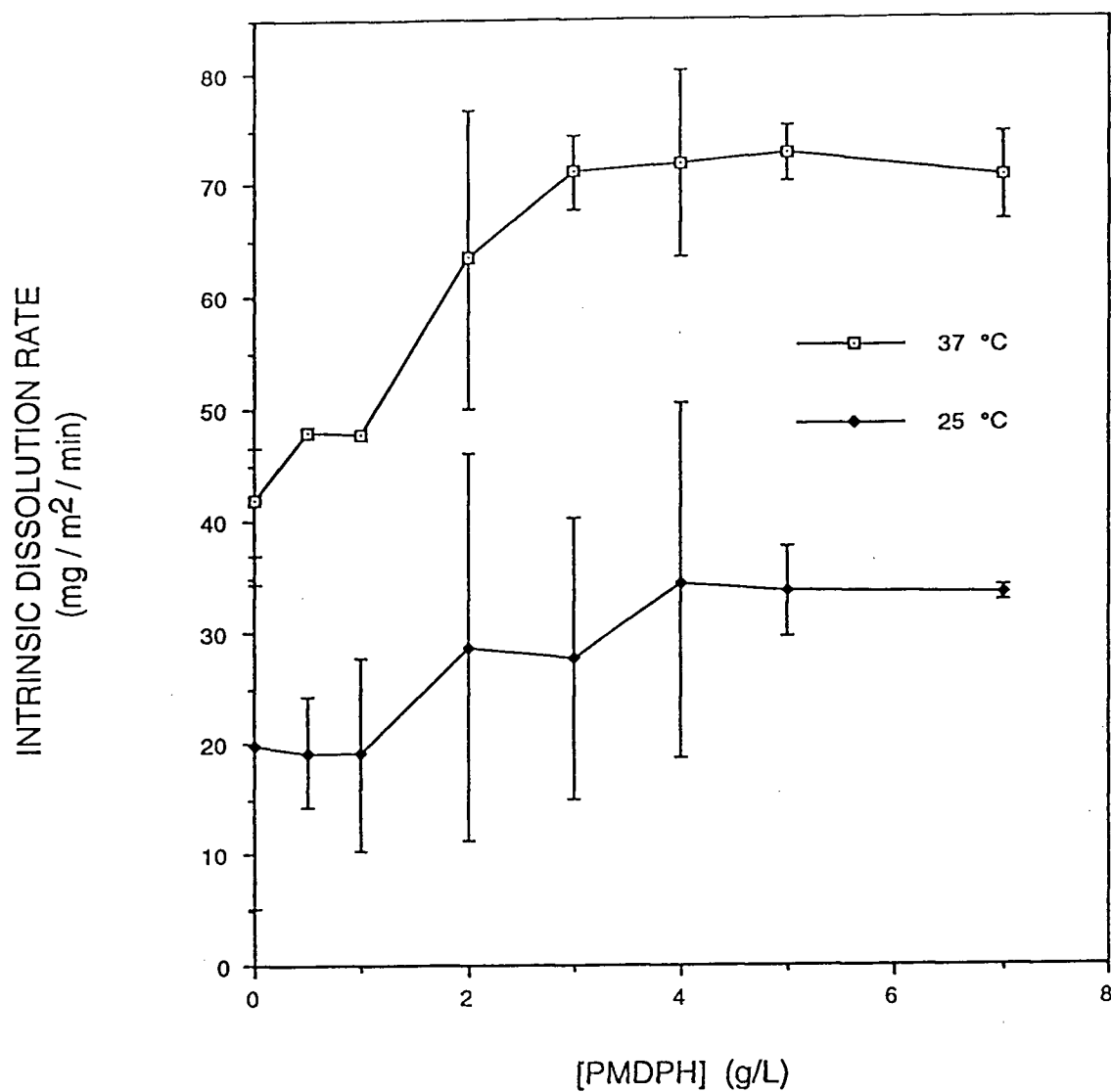


Fig. 28 Intrinsic dissolution rates at both 25 ° and 37 °C and at 100 rpm of DPH crystals grown from methanol containing various concentrations of PMDPH. The vertical bars represent the standard deviations of 6 determinations.

will not significantly affect the  $\Delta H^f$  of the DPH crystals although they may facilitate nucleation and may thus increase the number of 'active' sites available for dissolution. However, dislocation defects are defects of much larger magnitude and may generate considerable strain in the crystal lattice thereby influencing both the enthalpy of fusion (Swalin, 1972) and the dissolution rate (Burt and Mitchell, 1981) of the crystals.

On the other hand, the plateauing of IDR observed for samples prepared at 3 - 7 gL<sup>-1</sup> PMDPH may be ascribed to 'poisoning' of the active sites for dissolution in the crystals by adsorbed PMDPH (Piccolo and Tawashi, 1970, 1971a, 1971b) and to the relatively poor wettability of adsorbed PMDPH. These two factors, though theoretically operative at any concentration of PMDPH, are likely to gain dominance only when significantly high sorption of the additive has occurred.

#### 3.2.6.2 Effect of stirring speed on dissolution rate

The dissolution behavior of the various PMDPH-doped crystal samples was examined at 25 °C and at a stirring rate of 200 rpm. The increase in agitation rate from 100 to 200 rpm resulted in increases in the initial dissolution rates of the various samples to roughly the same extent such that the trends in dissolution rate at both stirring speeds almost paralleled each other (Fig. 27). To further examine the role of transport-mediated mechanisms of dissolution, the rates of dissolution of the crystals prepared at 0, 1 and 5 g L<sup>-1</sup> PMDPH were examined at 25 °C using stirring speeds varying between 50 and 250 rpm (Fig. 29). The IDRs of these samples were found to increase with the rate of stirring although the rate of increase appears to decline at higher stirring speeds (i.e., 150 rpm and above). Such a gradual rise in dissolution rate suggests that the dissolution process may be under both surface-reaction and transport control

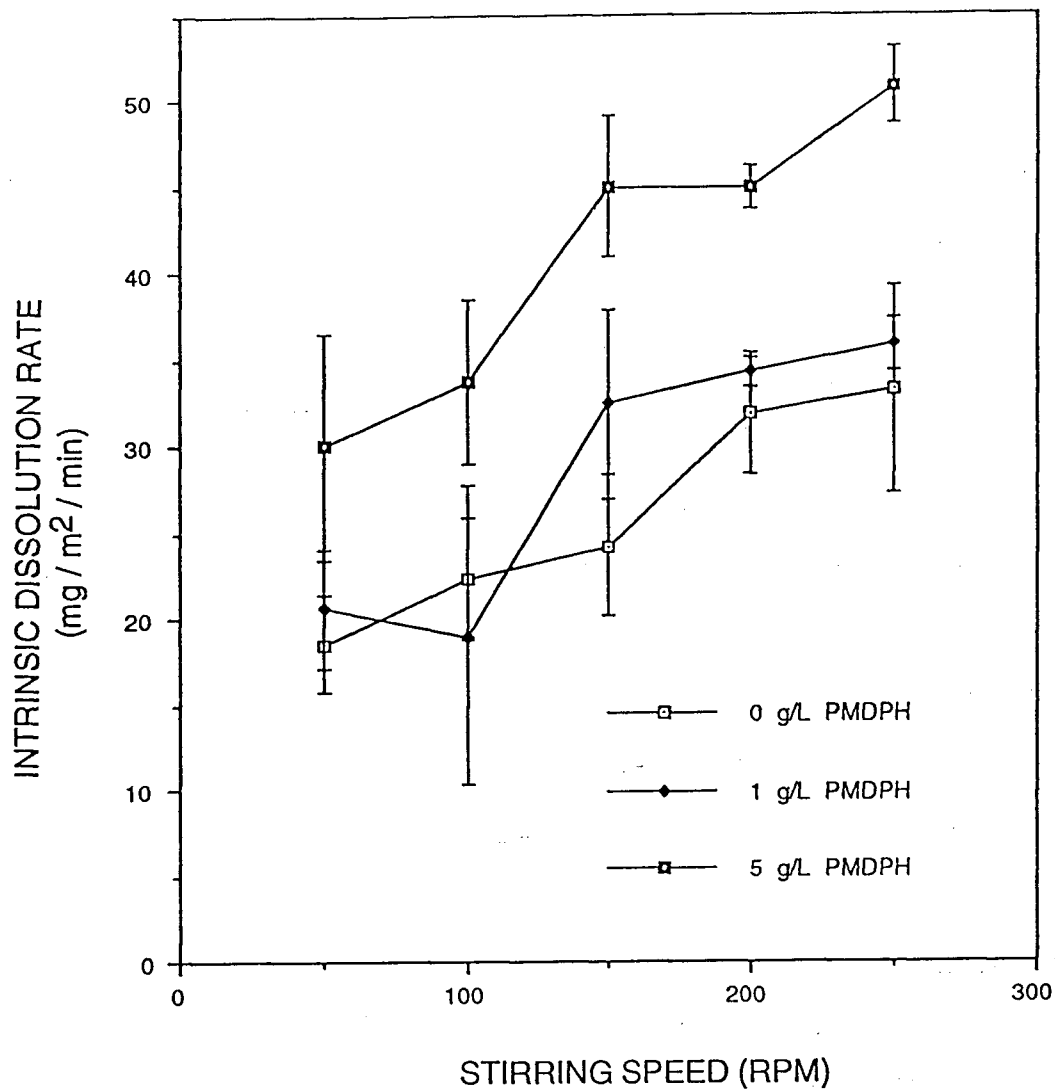


Fig. 29 Effect of stirring speed on the intrinsic dissolution rate of DPH crystals grown from methanol containing 0, 1 and 5 g L<sup>-1</sup> of PMDPH. The vertical bars represent the standard deviations of 6 determinations.

within the range of stirring speed employed. The IDR trends shown in Fig. 29 suggest that the dissolution process may be approaching the surface reaction controlled regime at higher rates of stirring. However, this could not be confirmed as 250 rpm is the upper limit of the stirring speed possible with the equipment employed in the present work.

### 3.2.6.3 Comparison with AMDPH-doped DPH samples

The present findings are similar to those previously obtained for AMDPH in many respects. Both additives yielded samples which exhibited maximal dissolution rates at intermediate concentrations of the additives in solutions with decreases (or plateauing) in rate at higher concentrations. While these results may indicate that both additives behave in a similar fashion at higher concentrations towards the dissolution process of DPH (i.e., they both can poison the active dissolution sites), the mechanisms involved may be different since the initial dissolution rates of the AMDPH-doped crystals showed no significant changes upon raising the stirring rate of the dissolution media from 100 to 200 rpm. The latter observations suggest that the dissolution rates of the AMDPH-doped samples are probably controlled by the surface properties of the DPH crystals rather than by the diffusion of solute away from the crystal surface, whereas the dissolution of the PMDPH-doped samples is both surface-reaction and diffusion-determined under the same conditions as evidenced by a gradual rise in dissolution rate with increasing stirring rate (Fig. 29).

#### 4. CONCLUSIONS

The following conclusions can be reached:

- (1) Growth of DPH crystals from methanol containing various concentrations of the additive, PMDPH, results in a linear rise in the sorption of PMDPH (0.03 – 0.57 mole %) as well as changes in the habit, particle size, specific surface area, fusion energetics and dissolution rate of the crystals.
- (2) Unlike AMDPH, PMDPH tends to adsorb predominantly on the surface of the DPH crystals.
- (3) As with AMDPH, the sorption of PMDPH reduces both the enthalpy of fusion,  $\Delta H^f$ , and entropy of fusion,  $\Delta S^f$ , of the crystals, corresponding to an increase in both the enthalpy and entropy of the crystals. The presence of PMDPH generates marginally less lattice disorder and disruption in the DPH crystals than does the presence of AMDPH, as determined by the relative magnitude of their disruption indices (i.e. the negative slopes of  $\Delta S^f$  versus  $\Delta S_{ideal}$ ) (Chow and Hsia, 1991).
- (4) As with previous studies employing AMDPH as the crystallization additive (Chow and Hsia, 1991), the observed changes in dissolution rate cannot be explained entirely in terms of the changes in surface area. The following factors probably play roles of differing significance: (a) defects on the surface and within the bulk of the crystals (induced by PMDPH and/or crystallization conditions); (b) crystal anisotropy; and (c) dissolution hydrodynamics. Though similar in many aspects towards the dissolution behavior of DPH, both AMDPH and PMDPH probably do not act via the same mechanism. The dissolution of AMDPH-treated crystals appears to be rate-limited by the surface properties of

the crystals while the dissolution of the PMDPH-doped samples seems to be both surface and diffusion-determined under the same experimental conditions.

(5) Like AMDPH, PMDPH has the ability to reproducibly modulate and enhance the intrinsic dissolution rate of DPH crystals.

(6) The present studies clearly demonstrate that a minor change in the structure of a homologous crystallization additive could significantly influence its interaction with the drug in the solid state and the resulting physicochemical properties.

## 5. SUGGESTIONS FOR FUTURE STUDIES

1. Since the additive appears to be unevenly distributed throughout the DPH crystals, as demonstrated by a large proportion (~70 %w/w) of the sorbed additive being found at or near the crystal surface, the location of the additive in the crystals will be studied by selective dynamic dissolution in a column-type glass cell using different solvents or mixtures of solvents of varying polarities. Such studies may provide some valuable insight into the dissolution mechanisms of the doped crystals.
2. The present work has clearly demonstrated the feasibility of systematically modifying the crystal habit and crystal defects of DPH using a crystallization additive related to the drug by structure. Since these crystal properties are known to play an important role in pharmaceutical processing (see Sections 1.2.3 and 1.3.4), a study of the effects of doping on the compact behavior of DPH may provide a better understanding of such a role.
3. Whether or not the methyl ester derivatives of DPH can form a true substitutional solid solution with DPH remains obscure. Future studies will focus on analysis of the crystal structures of doped DPH samples, AMDPH and PMDPH using single crystal X-ray crystallography. Solid-state nuclear magnetic resonance spectroscopy, which is complimentary to the X-ray diffraction technique, will also be employed to examine the solid state interactions between the additive and DPH. These studies may help determine whether the formation of a true substitutional solid solution is possible with DPH and the aforementioned additives, and if so, to what extent.



4. Since substantial changes in the morphology, surface features and dissolution rate of the crystals have been observed, a study of the surface energetics of the crystals may provide a better understanding of the mechanisms by which the additive exerts the observed effects. The surface tension of the crystals will be determined using the sedimentation technique developed by Vargha-Butler, Neumann et al. (1985, 1987) and/or calculated using an equation of state relation (Neumann, 1974) from the contact angles measured for droplets of a suitable wetting liquid with the surface of a compact made from compressed crystals.

5. Since significant enhancement of the dissolution rate of the DPH crystals doped with AMDPH or PMDPH has been observed, the bioavailability of these crystals in rats will be determined after oral administration (i.e., gastric intubation) to examine the potential of sorbed additives for modulating drug bioavailability.

## 6. REFERENCES

- Alderborn, G. and Nystrom, C., Studies on direct compression of tablets III. The effect on tablet strength of changes in particle shape and texture obtained by milling. *Acta Pharm. Suec.*, 19 (1982) 147-157.
- Arnold, K., Gerber, N., and Levy, G., Absorption and dissolution studies on sodium diphenylhydantoin capsules. *Can. J. Pharm. Sci.*, 5 (1970) 89-92.
- Berkovitch-Yellin, Z., Toward an *ab initio* derivation of crystal morphology. *J. Am. Chem. Soc.*, 107 (1985) 8239-8253.
- Berthoud, A., Theorie de la formation des faces d'un cristal. *J. Chim. Phys.*, 10 (1912) 624-635.
- Bircumshaw, L.L. and Riddiford, A.C., Transport control in heterogeneous reactions. *Q. Rev. Chem. Soc.*, 6 (1952) 157-185.
- Boldyrev, V.V., Bulens, M. and Delmon, B., *The control of the reactivity of solids*, Elsevier, New York, N.Y., 1979, p. 15.
- Brunner, E., Zur Kenntnis der Auflosungsgeschwindigkeit des Zinks. *Z. Phys. Chem.*, 51 (1905) 95-105.
- Bundgaard, H., Influence of acetylsalicylic anhydride impurity on the rate of dissolution of acetylsalicylic acid. *J. Pharm. Pharmac.*, 26 (1974) 535-540.
- Burt, H.M. and Mitchell, A.G., Dissolution anisotropy in nickel sulfate alpha-hexahydrate crystals. *Int. J. Pharm.*, 3 (1979) 261-274.
- Burt, H.M. and Mitchell, A.G., Effect of habit modification on dissolution rate. *Int. J. Pharm.*, 5 (1980) 239-251.
- Burt, H.M. and Mitchell, A.G., Crystal defects and dissolution. *Int. J. Pharm.*, 9 (1981) 137-182.

- Burton, W.K., Cabrera, N. and Frank, F.C., The growth of crystals and the equilibrium structure of their faces. *Phil. Trans.*, A243 (1951) 299-358.
- Byrn, S.R., *Solid State Chemistry of Drugs*, Academic Press, New York, N.Y., 1982.
- Chiou, W.L., Pharmaceutical applications of solid dispersion systems: X-ray diffraction and aqueous solubility studies on griseofulvin-polyethylene glycol 6000 systems. *J. Pharm. Sci.*, 66 (1977) 989-991.
- Chiou, W.L. and Kyle, L.E. Differential thermal, solubility, and aging studies on various sources of digoxin and digitoxin powder: Biopharmaceutical implications. *J. Pharm. Sci.*, 68 (1979) 1224-1229.
- Chow, A.H.-L., Chow, P.K.K., Wang Zhongshan and Grant, D.J.W., Modification of acetaminophen crystals: influence of growth in aqueous solutions containing *p*-acetoxyacetanilide on crystal properties. *Int. J. Pharm.*, 24 (1985) 239-258.
- Chow, A.H.-L. and Hsia, C.K., Modification of phenytoin crystals: influence of 3-acetoxymethyl-5,5-diphenylhydantoin on solution-phase crystallization and related crystal properties. *Int. J. Pharm.* (In press).
- Chow, A.H.-L., (1991) unpublished data.
- Chow, K.Y., Go, J., Mehdizadeh, M., and Grant, D.J.W., Modification of adipic acid crystals: influence of growth in the presence of fatty acid additives on crystal properties. *Int. J. Pharm.*, 20 (1984) 3-24.
- Davey, R.J., Adsorption of impurities at growth steps. *J. Crystal Growth*, 29 (1975) 212-214.
- Davey, R.J., The effect of impurity adsorption on the kinetics of crystal growth from solution. *J. Crystal Growth*, 34 (1976) 109-119.
- Davey, R.J., The control of crystal habit, in *Industrial Crystallization* 78. Ed. by de Jong, E.J. and Jancic, S.J. North-Holland Publishing Co., 1979.

- Desiraju, G.R., Designing organic crystals. *Prog. Solid St. Chem.*, 17 (1987) 295-353.
- El-Shattway, H.H., Kildsig, D.O. and Peck, G.E., Aspartame-mannitol resolidified fused mixture: Characterization studies of differential scanning calorimetry, thermomicroscopy, photomicrography and X-ray diffractometry. *Drug Dev. and Ind. Pharm.*, 10 (1984) 1-17.
- Fairbrother, J.E. and Grant, D.J.W., The crystal habit modification of a tablet lubricant, adipic acid. *J. Pharm. Pharmacol.*, 30 Suppl. (1978) 19P.
- Fairbrother, J.E. and Grant, D.J.W., Crystal engineering studies with an excipient material (adipic acid). *J. Pharm. Pharmacol.*, 31 Suppl. (1979) 27P.
- Frank, F.C., The influence of dislocations on crystal growth. *Discuss. Farad. Soc.*, 5 (1949) 48-54.
- Frank, S.C., *J. Pharm. Sci.*, 64 (1975) 1585.
- Gibaldi, M. and Feldman, S., Establishment of sink conditions in dissolution rate determinations. *J. Pharm. Sci.*, 56 (1967) 1238-1242.
- Gordon, J. and Chow, A.H.-L., Modification of phenytoin crystals: influence of 3-propanoyloxymethyl-5,5-diphenylhydantoin on solution-phase crystallization and related crystal properties. *Int. J. Pharm.* (In press).
- Haleblian, J. and McCrone, W., Pharmaceutical application of polymorphism. *J. Pharm. Sci.*, 58 (1969) 911-929.
- Haleblian, J.K., Characterization of habits and crystalline modification of solids and their pharmaceutical applications. *J. Pharm. Sci.*, 64 (1975) 1269-1288.
- Hartman, P., Crystal form and crystal structure, in physics and chemistry of the organic solid state, Ed. by Fox, D., Labes, M.M. and Weissberger, A., Vol. 1 (1963), chapter 6, 369-409.

- Higuchi, W.I., Lau, P.K., Higuchi, T. and Shell, J.W., Polymorphism and drug availability: Solubility relationships in the methylprednisolone system. *J. Pharm. Sci.*, 52 (1963) 150-153.
- Higuchi, W.I., Diffusional models useful in biopharmaceutics. *J. Pharm. Sci.*, 56 (1967) 315-324.
- Higuchi, W.I. and Simonelli, P.A., Particle phenomena, in Remington Pharmaceutical Science, 5th ed., Chapter 23, Mack, Pennsylvania, 1975, 340.
- Hull, D. and Bacon, D.J., Introduction to dislocations, Pergamon Press, Oxford, 1984, pp.13-20.
- Huttenrauch, R., The mechanism of tablet forming-a new conception. *Proc. 1st Inter. Conf. Pharm. Tech.*, Paris, 1977, Vol. IV, pp. 114-120.
- Huttenrauch, R., Molecular pharmaceutics as a basis for modern drug-forming. *Acta Pharm. Tech.*, Supplement, 6 (1978) 55-127.
- Huttenrauch, R., and Keiner, I., Einfluß des preßdrucks auf den ordnungsgrad von cellulosepulvren. *Pharmazie*, 31 (1976) 490-491.
- Huttenrauch, R., and Keiner, I., Producing lattice defects by drying processes. *Int. J. Pharm.*, 2 (1979) 59-60.
- Jachowicz, R., Dissolution rates of partially water-soluble drugs from solid dispersion systems. II. phenytoin. *Int. J. Pharm.*, 35 (1987) 7-12.
- Jamali, F. and Mitchell, A.G., The recrystallization and dissolution of acetylsalicylic acid. *Acta Pharm. Suec.*, 10 (1973) 343-352.
- Jones, T.M., The influence of physical characteristics of excipients on the design and preparation of tablets and capsules. *Pharm. Ind.*, 39 (1977) 469-476.

- Jones, S.P., and Grant, D.J.W., Cyclodextrins in the pharmaceutical sciences  
Part I: Preparation, structure and properties of cyclodextrin inclusion  
compounds. *Acta Pharm. Tech.*, 30 (1984a) 213-223.
- Jones, S.P., and Grant, D.J.W., Cyclodextrins in the pharmaceutical sciences  
Part II: Pharmaceutical, biopharmaceutical, biological and analytical  
aspects, and applications of cyclodextrin and its inclusion compounds.  
*Acta Pharm. Tech.*, 30 (1984b) 263-277.
- Kitaigorodsky, A.I. and Myasnikova, R.M., *Sov. Phys. Crystallogr.*, 5 (1960) 610.
- Kitaigorodsky, A.I., *Molecular Crystals and Molecules*, Academic Press Inc., NY,  
New York, 1973, pp. 95–105.
- Kitaigorodsky, A.I., *Mixed Crystals*, Springer-Verlag, Berlin, 1984.
- Klapper, H., Defects in non-metal crystals, in *Characterization of Crystal  
Growth by X-ray Methods*, Ed. by Tanner, B.K. and Bowen, D.K., Plenum  
Press, New York, 1979, 133-157.
- Kossel, W., Zur energetik von oberflachenvorgangen. *Annin Phys.*, 21 (1934)  
457.
- Levich, B.G., *Physicochemical Hydrodynamics*, Vol. II, Ed. by Spalding, D.B.,  
Advance Publications Ltd., London, 1977.
- Lieberman, H.A., and Lachman, L., *Pharmaceutical dosage forms-tablets*, Vol. I,  
Marcell Decker, New York, 1980.
- Lowell, S., Continuous flow krypton adsorption for low surface area  
measurements. *Analytical Chem.*, 45 (1973), 1576.
- Menard, F.A., Dedhiya, M.G., and Thodes, C.T., Studies of the effect of pH,  
temperature and ring size on the complexation of phenytoin with  
cyclodextrins. *Pharm. Acta Helv.*, 63 (1988) 303-308.
- Michaels, A.S., and Colville, A.R., The effect of surface active agents on crystal  
growth rate and crystal habit. *J. Phys. Chem.*, 64 (1960) 13-19.

- Mitchell, A.G. and Saville, D.J., The dissolution of commercial aspirin. *J. Pharm. Pharmac.*, 21 (1969) 28-34.
- Mitchell, A.G., Milaire, B.L., Saville, D.J. and Griffith, R.V., Aspirin dissolution: Polymorphism, crystal habit or crystal defects. *J. Pharm. Pharmac.*, 23 (1971) 534-535.
- Moore, W.J., *Physical Chemistry*, 4th ed., Prentice-Hall, Inc., Englewood Cliffs, N.J., USA, 1972, p.883.
- Mullin, J.W., *Crystallization*, CRC Press, Cleveland, Ohio, 1972.
- Nernst, W., Theorie der reaktionsgeschwindigkeit in heterogenen systemen. *Z. Phys. Chem.*, 47 (1904) 52-102.
- Neumann, A.W., Good, R.J., Hope, C.J. and Sejpal, M., An equation-of-state approach to determine surface tensions of low-energy solids from contact angles. *Journal of Colloid and Interface Science*, 49 (1974) 291-304.
- Noyes, A.A. and Whitney, W.R., The rate of solution of solid substances in their own solutions. *J. Am. Chem. Soc.*, 19 (1897) 930-934.
- Phillip, J., Holcomb, I. J., and Fusari, S. A., Phenytoin. Analytical profiles of drug substances (Vol. 13), A. P. A. Press, Orlando, FLA, (1984).
- Piccolo, J. and Tawashi, R., Inhibited dissolution of drug crystals by a certified water soluble dye. *J. Pharm. Sci.*, 59 (1970) 56-59.
- Piccolo, J. and Tawashi, R., Inhibited dissolution of drug crystals by certified water soluble dyes. II. *J. Pharm. Sci.*, 60 (1971a) 59-63.
- Piccolo, J. and Tawashi, R., Inhibited dissolution of drug crystals by certified water soluble dyes. III. *J. Pharm. Sci.*, 60 (1971b) 1818-1820.
- Pikal, M.J. and Grant, D.J.W., A theoretical treatment of changes in energy and entropy of solids caused by additives or impurities in solid solution. *Int. J. Pharm.*, 39 (1987) 243-253.

- Pilpel, N., in Rawlins E.A. (ed.) Bentley's Textbook of Pharmaceutics, 8th Edn., Bailliere Tindall, London, 1977, p.234.
- Rail, L., "Dilantin" overdose. Med. J. Aust., 2 (1968) 339.
- Ridgway, K. and Rupp, R., The effect of particle shape on powder properties. J. Pharm. Pharmac., Suppl., 21 (1969) 30S-39S.
- Ridgway, K. and Shotton, J.B., The effect of particle shape on the variation of fill of a tableting die. J. Pharm. Pharmac., Suppl., 22 (1970) 24S-28S.
- Sekikawa, H., Fujiwara, J., Naganuma, T., Nakano, M., and Arita, T., Dissolution behaviors and gastrointestinal absorption of phenytoin in phenytoin-polyvinyl pyrrolidone coprecipitate. Chem. Pharm. Bull., 26(1978) 3033-3039.
- Simmons, D.L., Ranz, R.J., Gyanchandani, N.D., and Picotte, P., Polymorphism in pharmaceuticals II: Tolbutamide. Can. J. Pharm. Sci., 7 (1972) 121-123.
- Stella, V., Higuchi, T., Hussain, A. and Truelove, J., in *Prodrugs as novel drug delivery systems*. Ed. by Higuchi, T. and Stella, V., American Chemical Society Symposium Series 14 (1975) 154-183.
- Swalin, R.A., Thermodynamics of solids, John Wiley & Sons, Inc., New York, 1962.
- Uekama, K., Otagiri, M., Irie, T., Seo, H., and Tsuruoka, M., Improvement of dissolution and absorption characteristics of phenytoin by a water-soluble  $\beta$ -cyclodextrin-epichlorohydrin polymer. Int. J. Pharm., 23 (1985) 35-42.
- Valeton, J.J.P., Wachstum und auflosung der kristalle. Z. Kristallogr., 59 (1923) 135, 335.
- Valeton, J.J.P., Wachstum und auflosung der kristalle. Z. Kristallogr., 60 (1924) 1.



- Vargha-Butler, E.I., Zubovits, T.K., Absolom, D.R., Neumann, A.W. and Hamza, H.A., Surface tension effects in the sedimentation of coal particles in various liquid mixtures. *Chem. Eng. Commun.*, 33 (1985) 255-276.
- Vargha-Butler, E.I., Moy, E. and Neumann, A.W., Sedimentation behavior of low surface energy powders in different non-polar liquid systems. *Colloids and Surfaces*, 24 (1987) 315-324.
- Varia, S.A., Schuller, S., Sloan, K.B. and Stella, V.J., Phenytoin prodrugs III: water-soluble prodrugs for oral and/or parenteral use. *J. Pharm. Sci.*, 73 (1984a) 1068–1073.
- Varia, S.A., Schuller, S. and Stella, V.J., Phenytoin prodrugs IV: Hydrolysis of various 3-(hydroxymethyl)phenytoin esters. *J. Pharm. Sci.*, 73 (1984b) 1074.
- Varia, S.A. and Stella, V.J., Phenytoin prodrugs V: *In vivo* evaluation of some water-soluble phenytoin prodrugs in dogs. *J. Pharm. Sci.*, 73 (1984a) 1080.
- Varia, S.A. and Stella, V.J., Phenytoin prodrugs VI: *In vivo* evaluation of a phosphate ester prodrug of phenytoin after parenteral administration to rats. *J. Pharm. Sci.*, 73 (1984b) 1087.
- Volmer, M., *Kinetik der phasenbildung*, Dresden and Leipzig, Steinkopff, 1939.
- Volmer, M., and Schultz, W., Kondensation an kristallen. *Z. Phys. Chem.*, 156 (1931) 1.
- Watanabe, A., Yamaoka, Y. and Takada, K., Crystal habits and dissolution behavior of aspirin. *Chem. Pharm. Bull.*, 30 (8) (1982) 2958-2963.
- Wurster, D.E. and Taylor, P.W., Dissolution kinetics of certain crystalline forms of prednisolone. *J. Pharm. Sci.*, 54 (1965a) 670-676.
- Wurster, D.E. and Taylor, P.W., Dissolution rates. *J. Pharm. Sci.*, 54 (1965b) 169-175.

- Yakou, S., Umehara, K., Sonobe, T., Nagai, T., Sugihara, M., and Fukuyama, Y., Particle size dependency of dissolution rate and human bioavailability of phenytoin in powders and phenytoin-polyethylene glycol solid dispersions. *Chem. Pharm. Bull.*, 32 (1984) 4130-4136.
- Yakou, S., Yamazaki, S., Sonobe, T., Sugihara, M., Fukumoro, K., and Nagai, T., Particle size distribution affects the human bioavailability of phenytoin. *Chem. Pharm. Bull.*, 34 (1986) 4400-4402.
- Yamaoka, Y., Roberts, R.D. and Stella, V.J., Low-melting phenytoin prodrugs as alternative oral delivery modes for phenytoin: A model for other high-melting sparingly water-soluble drugs. *J. Pharm. Sci.*, 72 (1983) 400.
- York, P., Particle slippage and rearrangement during compression of pharmaceutical powders. *J. Pharm. Pharmac.*, 30 (1978) 6-10.
- York, P., Solid-state properties of powders in the formulation and processing of solid dosage forms. *Int. J. Pharm.*, 14 (1983) 1-28.
- York, P. and Grant, D.J.W., A disruption index for quantifying the solid state disorder induced by additives or impurities. 1. Definition and evaluation from heat of fusion. *Int. J. Pharm.*, 25 (1985) 57-72.